ined for construction of carbosilane dendrimers uniformly functionalized with *N*-acetyllactosamine residues through thioglycoside linkages. The incorporation of *N*-acetyllactosamine residues into a carbosilane **7**[11] under conditions similar to those used for the preparation of **6** proceeded smoothly and gave the corresponding glycocluster **8** in 68.7% yield (Scheme 3), $[\alpha]_D^{23}$ −39.9° (*c* 0.093, $CHCl_3$), integral ratio of the H atoms by $^1H$ NMR: $SiCH_2$:$SCH_2$:Ph:H-1′ = 6:6:5:3, FABMS calcd for [M+H$^+$]: 2183.69; Found *m/z*: 2183.62. An analogue of the thioglycoside-type glycocluster was also prepared in a manner similar to that used for the preparation of **4** using triol **9**[14] as a cluster-type alcohol to provide glycocluster **10** in 33.0% yield, $[\alpha]_D^{28}$ −14.2° (*c* 0.427, MeOH), integral ratio of the H atoms by $^1H$ NMR: $SiCH_2$:Ph:H-1′ = 6:5:3, FABMS calcd for [M+H$^+$]: 2135.76; Found *m/z*: 2135.50, which was an attractive compound in comparison with thioglycoside-type glycocluster for activity against glysosidase and glycosyltransferase, respectively. Finally, the protected glycoclusters **8** and **10** were quantitatively deprotected by a combination of typical Zemplén's manner and saponification to afford corresponding water soluble **11**, IR 1652 (Amide I; $\nu_{C=O}$) and 1558 (Amide II; $\delta_{N-H}$) cm$^{-1}$, FABMS calcd for [M+H$^+$]: 1426.50; Found *m/z*: 1426.41, and **12**, IR 1649 ($\nu_{C=O}$) and 1556 ($\delta_{N-H}$) cm$^{-1}$, FABMS calcd for [M+H$^+$]: 1378.57; Found *m/z*: 1378.40, respectively.

In conclusion, we have successfully demonstrated the preparation of a novel thioacetate **2** of *N*-acetyllactosamine and the efficient activation of **2** for glycoside synthesis yielding a couple of glycosides through an *O*- or *S*-glycosidic linkage, respectively. Further transformations of **2**, including synthetic assembly of **2** using other carbosilane dendrimers as core scaffolds and enzymatic elongation of sialic acid for the cluster-type compounds, are now in progress, and the results will be reported elsewhere.

## Acknowledgements

This work was partly supported by a Grant-in-Aid for Encouragement of Young Scientists (12750754) from the Ministry of Education, Science, and Culture of Japan (K.M.) and by a grant from NEDO [New

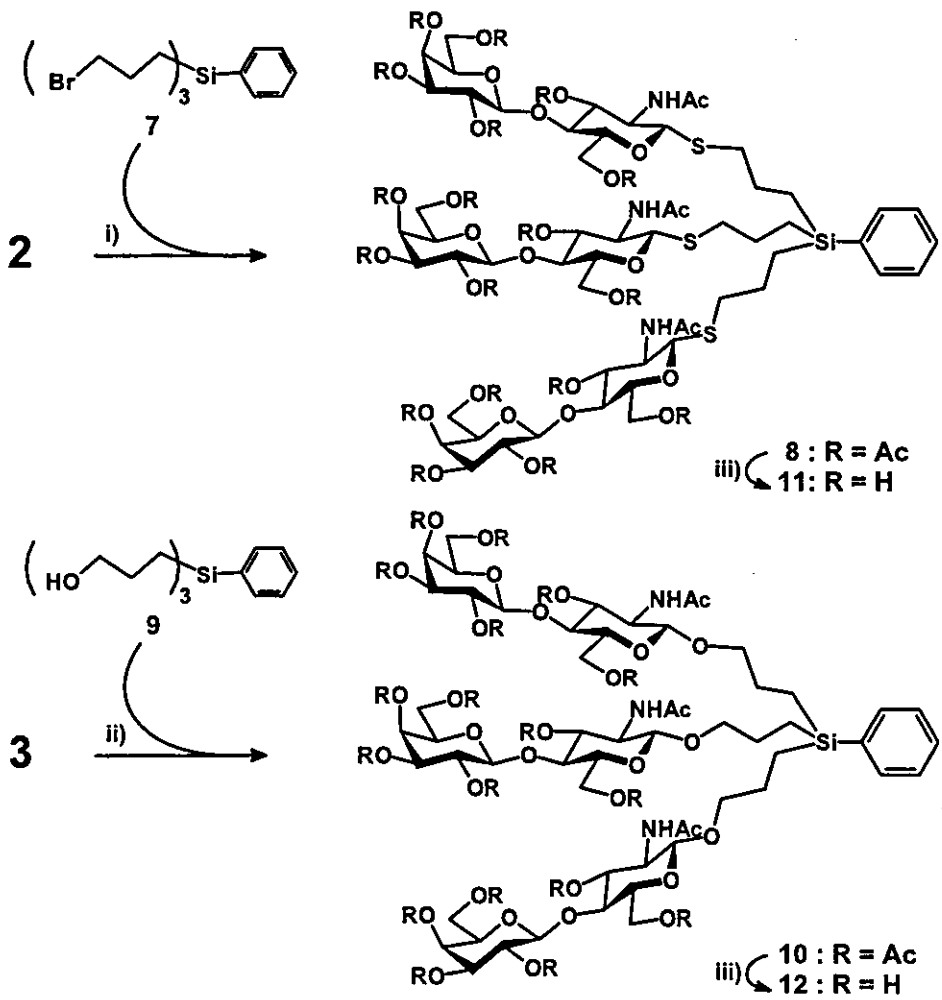


Scheme 3. *Reagents and conditions*: (i) NaOMe, MeOH, −40°C, then **7** (Ref. 11), −40°C, overnight, then $Ac_2O$–Pyr, rt; (ii) **9** (Ref. 14), CSA, $CH_2ClCH_2Cl$, 90°C.

Energy and Industrial Technology Development Organization (Glycocluster project)].

## References


1. For example, see: Fukuda, M.; Kobata, A. *Glycobiology*; IRL Press: Oxford, 1993 and references cited therein.
2. For example, see: (a) Nicolaou, K. C.; Caulfield, T. J.; Kataoka, H.; Stylianides, N. A. *J. Am. Chem. Soc.* **1990**, *112*, 3693–3695; (b) Kameyama, A.; Ishida, H.; Kiso, M.; Hasegawa, A. *Carbohydr. Res.* **1991**, *209*, c1–c4; (c) Nicolaou, K. C.; Hummel, C. W.; Vockovich, N. J.; Wong C.-H. *J. Chem. Soc., Chem. Commun.* **1991**, 870–872; (d) Nishimura, S.-I.; Murayama, S.; Kurita, K.; Kuzuhara, H. *Chem. Lett.* **1992**, 1413–1416; (e) Ball, E. G.; O'Neill, R. A.; Schultz, J. E.; Lowe, J. B.; Weston, B. W.; Nagy, J. O.; Brown, E. G.; Hobbs, C. J.; Bednarski, M. D. *J. Am. Chem. Soc.* **1992**, *114*, 5449–5451 and references cited therein.
3. Lemieux, R. U.; Ratcliffe, R. M. *Can. J. Chem.* **1979**, *57*, 1244–1251.
4. Rosen, T.; Lico, I. M.; Chu, D. T. W. *J. Org. Chem.* **1988**, *53*, 1580–1582.
5. (a) Bielfeldt, T.; Peters, S.; Meldal, M.; Bock, K.; Paulsen, H. *Angew. Chem., Int. Ed. Engl.* **1992**, 857–859; (b) Nakahara, Yo.; Nakahara, Yu.; Ogawa, T. *Carbohydr. Res.* **1996**, *292*, 71–81; (c) Chen, X.-T.; Sames, D.; Danishefsky, S. J. *J. Am. Chem. Soc.* **1998**, *120*, 7760–7769.
6. Garegg, P. J. *Adv. Carbohydr. Chem. Biochem.* **1997**, *52*, 179–205.
7. Yoshino, T.; Sato, K.-I.; Wanme, F.; Takaki, I.; Ishido, Y. *Glycoconjugate J.* **1992**, *9*, 287–291.
8. Nishimura, S.-I.; Matsuoka, K.; Furuike, T.; Ishii, S.; Kurita, K.; Nishimura, K. M. *Macromolecules* **1991**, *24*, 4236–4241.
9. Hasegawa, A.; Nakamura, J.; Kiso, M. *J. Carbohydr. Chem.* **1986**, *5*, 11–19.
10. (a) Matsuoka, K.; Terabatake, M.; Saito, Y.; Hagihara, C.; Esumi, Y.; Terunuma, D.; Kuzuhara, H. *Bull. Chem. Soc. Jpn.* **1998**, *71*, 2709–2713; (b) Matsuoka, K.; Saito, Y.; Terunuma, D.; Kuzuhara, H. *Kobunshironbunsyu* **2000**, *57*, 691–695.
11. Matsuoka, K.; Terabatake, M.; Esumi, Y.; Terunuma, D.; Kuzuhara, H. *Tetrahedron Lett.* **1999**, *40*, 7839–7842.
12. Matsuoka, K.; Kurosawa, H.; Esumi, Y.; Terunuma, D.; Kuzuhara, H. *Carbohydr. Res.* **2000**, *329*, 765–772.
13. Matsuoka, K.; Oka, H.; Koyama, T.; Esumi, Y.; Terunuma, D. *Tetrahedron Lett.* **2001**, *42*, 3327–3330.
14. Terunuma, D.; Kato, T.; Nishio, R.; Matsuoka, K.; Kuzuhara, H.; Aoki, Y.; Nohira, H. *Chem. Lett.* **1998**, 59–60.

高分子論文集 (Kobunshi Ronbunshu), Vol. 60, No. 10, pp. 561—568 (Oct., 2003)

# 新規カルボシランデンドリマーの合成とその構造が液晶性に与える効果

土田 隆樹[*1]・島崎 智恵美[*1]・幡野　健[*1]・松岡 浩司[*1]
青木 良夫[*1]・野平 博之[*1]・江角 保明[*2]・照沼 大陽[*1]

(受付 2003 年 5 月 16 日・審査終了 2003 年 7 月 17 日)

要　旨　3 種類の末端にシアノビフェニル基を有する分岐数が異なる第 2 世代カルボシランデンドリマー (Me$_n$G 2-Mesogen, n=1, 2, 3) を合成した．また，中心から外に向かって炭素鎖数が 2, 3, 4 と増加する傾斜型第 2 世代カルボシランデンドリマー (GradientG 2-Mesogen) を合成した．それぞれのシアノビフェニル基担持カルボシランデンドリマーについて示差走査熱量分析 (DSC) および偏光顕微鏡観察を行った．合成した四つのシアノビフェニル基担持第 2 世代カルボシランデンドリマーはすべてスメクチック A 相を示し，デンドリマーの構造が相転移温度および液晶ドメインサイズに対し強く影響することがわかった．また，液晶性傾斜型デンドリマーは相転移温度および液晶ドメインサイズともにデンドリマーを形成する炭素数がすべて 3 個のもの (G 2-Mesogen)[4] とほぼ同じであった．

## 1 緒　　言

従来の線状あるいは網状高分子とは，骨格が異なる巨大分子であるデンドリマーが注目を集めている[1]．デンドリマーは定まった分子量を有する巨大分子である．従来機能性高分子としては線状あるいは網目状高分子が検討されてきた．その場合高分子側鎖に導入された機能性基の働きが，その分子量分布あるいは立体配置などさまざまな要因によって影響をうけるため，均一性および再現性に問題が生じることがある．その点デンドリマー末端に機能性基を導入した場合には，分子量および分子サイズが正確に定まっておりすべての機能性基が分子表面に均一に配置され，結果として均一な機能の作用場を実現できる．さらに，デンドリマーに機能性基を導入した化合物はその分子量が大きいにもかかわらず一般に溶解性が良い．これらの特徴は高分子（巨大分子）を機能材料として利用する際に問題となる反応の不均一性を改善し，機能性基の集積化効果を観測することを可能とする．

デンドリマーは各世代の伸張に伴い枝部分の分岐を行うが，その分岐部分の原子（分子）としては窒素，ケイ素，ゲルマニウムあるいはベンゼンなどが報告されている[2]．筆者らはケイ素を分岐原子とするカルボシランデンドリマーを用いてその機能化を試みているが，カルボシランデンドリマーは世代伸張が比較的容易で安定な化合物であり種々の機能性基の導入が可能である．また，分岐原子となるケイ素上の官能基数を変えることにより分岐数を 1 から 3 までの範囲で容易に制御できることから，機能発現に最適な分子の設計に柔軟に対処可能という特徴も備えている[3]．

Lorenz らはテトラアリルシランをコア分子として第 2 世代カルボシランデンドリマーを合成し，そこにメソゲン基を導入することにより液晶性を示すカルボシランデンドリマーを調製しその物性について報告している[4]．筆者らは，これまでトリアリルフェニルシランをコア分子として合成したカルボシランデンドリマーを用いて，スペーサー長が液晶性に与える効果あるいは強誘電性液晶分子の導入によるカルボシランデンドリマーの効果について検討してきた[5]．

本研究ではカルボシランデンドリマー骨格が液晶性に与える効果を調べるため 3 種類のコア分子を用いた第 2 世代カルボシランデンドリマー (MeG 2-Mesogen, Me$_2$G 2-Mesogen, Me$_3$G 2-Mesogen) および枝の鎖長（メチレン鎖）が内側から 2, 3, 4 と増加する傾斜型第 2 世代デンドリマー (GradientG 2-Mesogen) (Fig. 1) を合成し，その物性について検討した．

## 2 結果と考察

### 2.1 合成

文献記載の方法[5] に準じてトリアリルメチルシラン，ジアリルジメチルシラン，アリルトリメチルシランを用いて世代拡張反応，すなわちヒドロシレーション，アリ

*1 埼玉大学工学部 (〒338-8570 さいたま市桜区下大久保 255)
*2 理化学研究所 (〒351-0106 和光市広沢 2-1)

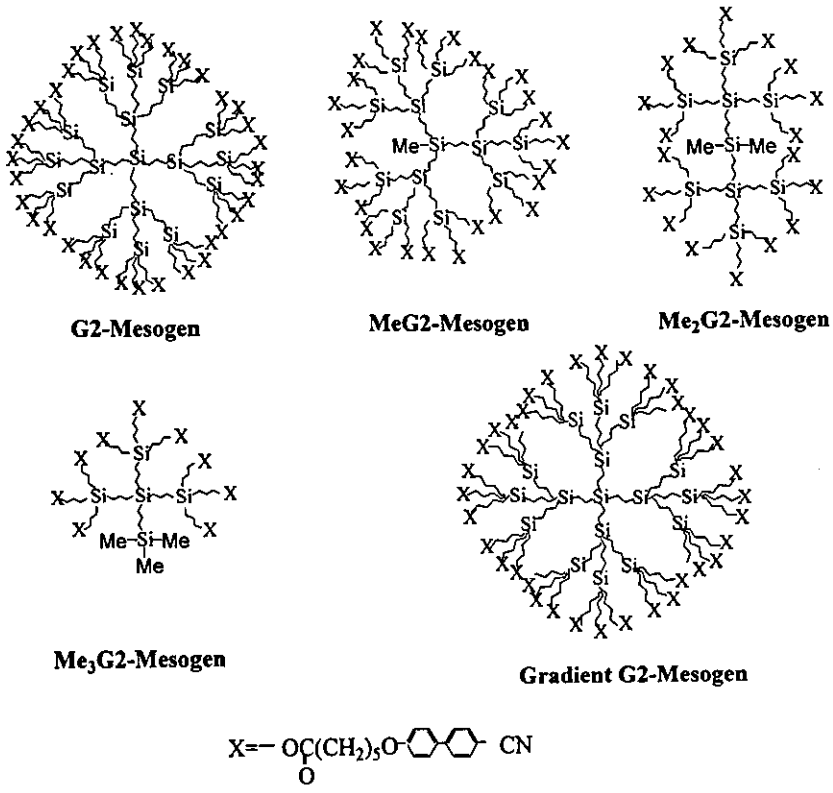


**Fig. 1.** Carbosilane dendrimers carrying mesogens.

ル化を2度繰返すことにより末端に二重結合を有する相当する第2世代カルボシランデンドリマーを合成した．それらにヒドロボレーションによりヒドロキシル基を導入した後シアノビフェニル誘導体を作用させてそれぞれ目的とする $Me_nG$ 2-，$Me_2G$ 2-および $Me_3G$ 2-Mesogen を合成した（Fig. 2）．

一方，内側から炭素鎖が2，3，4と増加する傾斜型デンドリマーを合成することを目指して，テトラビニルシランにヒドロシレーション，引き続きアリル化し，さらにヒドロシレーションした後過剰のブテニルグリニャール試薬を作用させて，その合成を試みたが，それぞれの末端ケイ素に3個のブテニル基を完全に導入した化合物を得ることはできなかった（Scheme 1）．第2世代クロロシランに対する置換反応が，その立体障害が強いことにより十分に進行しないためと考えられる．

そこでブテニルグリニャール試薬に代えて，まずアリルグリニャール試薬を作用させて3個のメチレン部分を導入し，その後炭素1個を増炭する経路により傾斜型デンドリマーの合成を試みた．すなわち第2世代のアリル基をヒドロボレーション，メシル化した後シアン化ナトリウムを作用させて炭素を一つ増加させシアノ誘導体を得た．さらにシアノ基の加水分解エステル化，水素化リチウムアルミニウムによる還元を経て末端にヒドロキシル基を有する傾斜型デンドリマーを合成した．それにシアノビフェニル誘導体を作用させて液晶分子を有する傾斜型第2世代デンドリマー（GradientG 2-Mesogen）を得ることができた（Scheme 2）．以上合成したシアノビフェニル担持第2世代デンドリマーは，いずれも通常の有機溶媒に可溶であった．

なお，内側から外側に向けて炭素鎖数が4，3，2と減少する傾斜型デンドリマーの合成についても検討したが，第2世代に相当するビニルグリニャール試薬との反

$MeSi(CH_2CH_2CH_2Si(CH_2CH_2CH_2Si(CH_2CH_2CH_2X)_3)_3)_3$

**MeG2-Mesogen**

$Me_2Si(CH_2CH_2CH_2Si(CH_2CH_2CH_2Si(CH_2CH_2CHX_2)_3)_3)_2$

**$Me_2$G2-Mesogen**

$Me_3Si(CH_2CH_2CH_2Si(CH_2CH_2CH_2Si(CH_2CH_2CH_2X)_3)_3$

**$Me_3$G2-Mesogen**

X = -OC(=O)(CH2)5O— CN

**Fig. 2.** Preparation of **$Me_nG$ 2-Mesogen** (n=1, 2, 3).

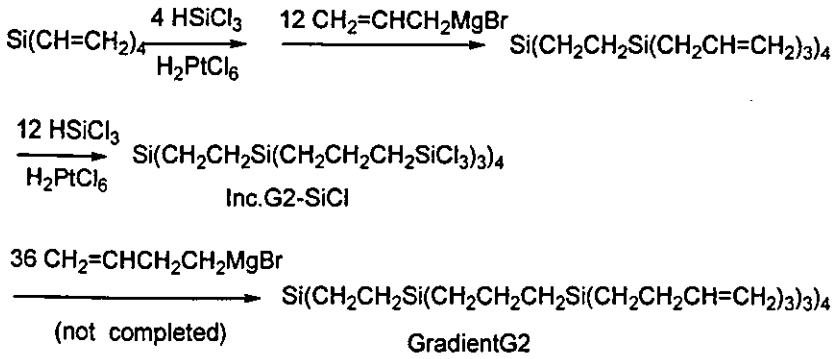


**Scheme 1.** An attempt at the preparation of Gradient G 2.

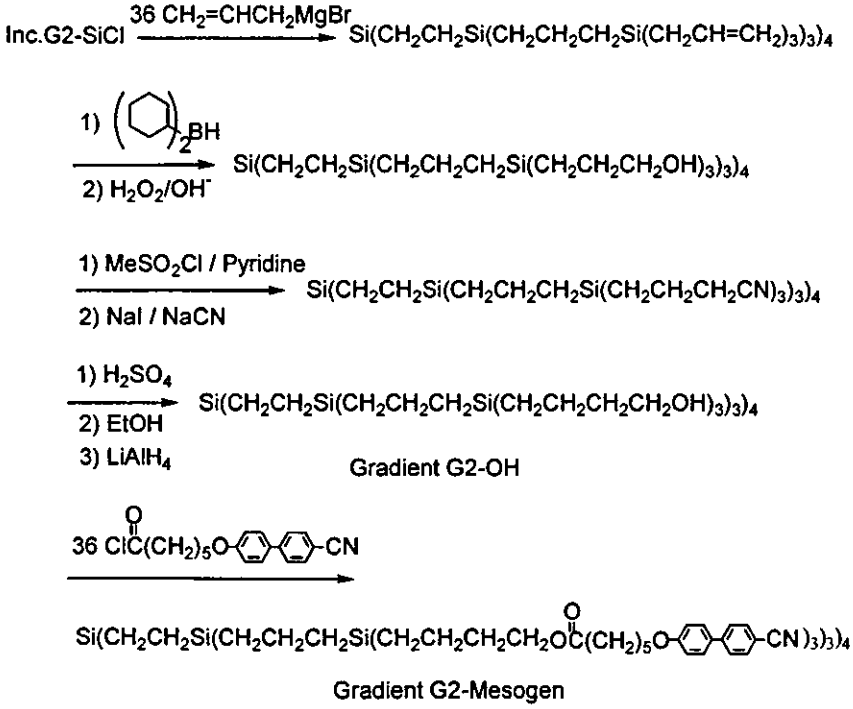


**Scheme 2.** Preparation of Gradient G 2-Mesogen.

応が完全には進行せず目的物を得るには至らなかった．

### 2.2 物性評価

今回合成したデンドリマーには，末端に導入されているシアノビフェニル基の数が $Me_1G$ 2-，$Me_2G$ 2-および $Me_3G$ 2-Mesogen の順に減少することから集積度が異なり，それぞれの化合物の液晶性が変化する可能性がある．それぞれの化合物の DSC チャートを Fig. 3 に，その解析結果を Table 1，2 に示す．また，偏光顕微鏡で観察した液晶相の写真を Fig. 4 に示す．

いずれの場合もガラス転移点は 10 ℃ 付近であり透明点は $Me_1G$ 2-，$Me_2G$ 2-および $Me_3G$ 2-Mesogen の順，すなわち集積度が小さくなるに従って低くなることがわかった．この傾向は，すでに報告されているテトラアリルシランをコア分子に用いた第 2 世代の液晶性カルボシランデンドリマー（G 2-Mesogen）[4] の場合のガラス転移点が 15 ℃，透明点が 130 ℃ であることとも整合する．また，$Me_1G$ 2-Mesogen と $Me_3G$ 2-Mesogen は狭い温度範囲で透明点を与えるのに対して，$Me_2G$ 2-Mesogen は広い温度範囲にわたり複雑な相転移を経て透明点にいたることが示された．また，偏光顕微鏡観察の結果は集積度が上昇するに従ってより大きな形状のドメインを与えることがわかった．これらの原因については明らかではないが，カルボシランデンドリマーの構造が液晶性に対して単に集積度の効果のみではなく，分子の対称性などが影響していることも考えられる．

一方，傾斜型カルボシランデンドリマーの場合，集積

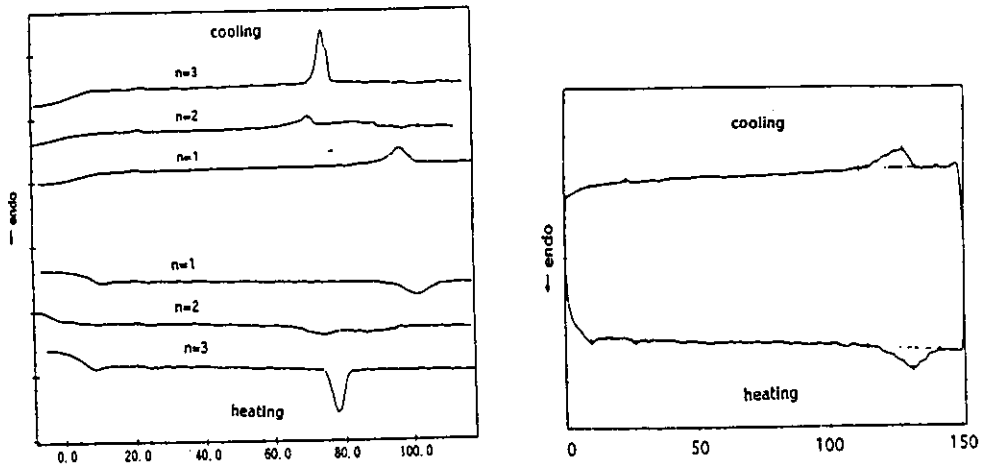


(a) $Me_nG$ 2-Mesogen (n=1, 2, 3) (b) Gradient G 2-Mesogen

**Fig. 3.** DSC chart of **$Me_nG$ 2-Mesogen** (n=1, 2, 3) (a) and **Gradient G 2-Mesogen** (b).

**Table 1.** Thermal behavior of **$Me_nG$ 2-Mesogen** (n=1, 2, 3)

| n | Phase behavior/℃ | | | | | | | | | |
|---|---|---|---|---|---|---|---|---|---|---|
| | Cooling | | | | | Second heating | | | | |
| 1 | I[a] | 97 | $S_A$[c] | 9 | G[b] | G | 11 | $S_A$ | 101 | I |
| 2 | I | 89 | $S_A$ | 8 | G | G | 10 | $S_A$ | 87 | I |
| 3 | I | 75 | $S_A$ | 9 | G | G | 9 | $S_A$ | 78 | I |

[a] I, isotropic; [b] G, Glass transition temperature; [c] $S_A$, smectic A.

**Table 2.** Thermal behavior of **Gradient G 2-Mesogen**

| Phase behavior/℃ | | | | | | | | | |
|---|---|---|---|---|---|---|---|---|---|
| Cooling | | | | | Second heating | | | | |
| I[a] | 128 | $S_A$[c] | 6 | G[b] | G | 8 | $S_A$ | 131 | I |

[a] I, isotropic; [b] G, Glass transition temperature; [c] $S_A$, smectic A.

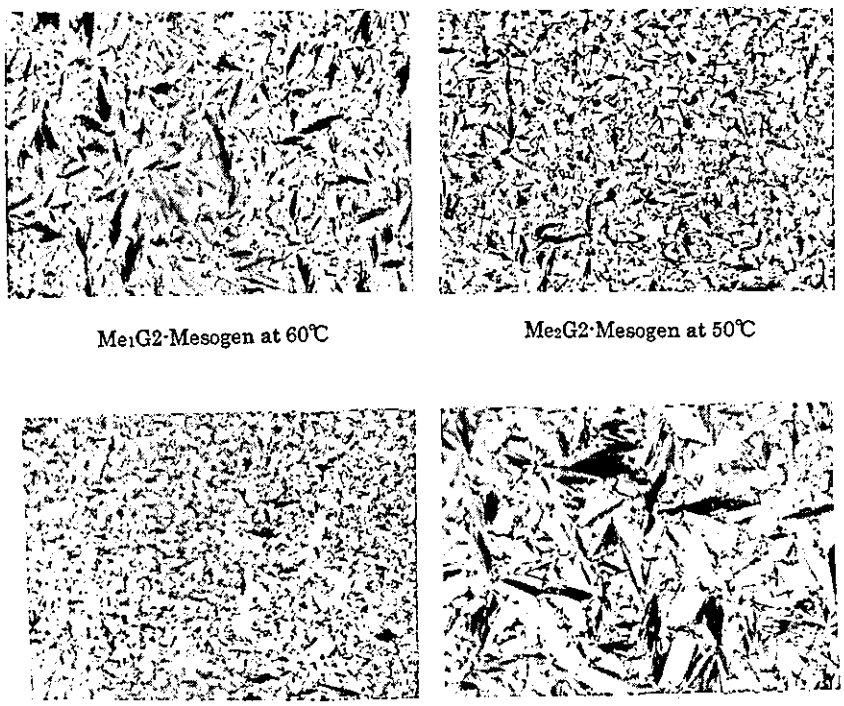

$Me_1G2$-Mesogen at 60℃ $Me_2G2$-Mesogen at 50℃

$Me_3G2$-Mesogen at 50℃ Gradient G2-Mesogen at 120℃

**Fig. 4.** Texture of **$Me_nG$ 2-Mesogen** (n=1, 2, 3) and **Gradient G 2-Mesogen** crossed polarizers.

度および総計のメチレン鎖長が同じG 2-Mesogen[3]と比較すると，ガラス転移点は若干低温側になるものの透明点はほとんど同じであった．また，偏光顕微鏡観察によっても両者のドメインの形状およびサイズはほぼ同じとなることがわかった．

## 3 実験方法

### 3.1 測定

$^1$H NMRおよび$^{13}$C NMRはBruker Inc.製AM 400, ARX 400およびVarian Inc.製Gemini 200を用いて測定した．IRおよびUVスペクトルは日本分光(株)製FT/IR-300 Eおよび JASCO V 550を用いてそれぞれ測定した．リサイクルGPC分取は日本分析工業(株)製LC-918 Rを用いて行った．偏光顕微鏡観察は(株)ニコン製Nikon Optiphot 2-Polを用いた．DSCは(株)マック・サイエンス製DSC 3100を使用した．

### 3.2 試薬

エーテルおよびテトラヒドロフラン（THF）はナトリウム上で乾燥後使用した．そのほかの試薬は市販品をそのまま使用した．

### 3.3 実験

**3.3.1 Me$_1$G 2-Mesogenの合成** アルゴン置換したフラスコにMe$_1$G 2-OH 90 mg（0.036 mmol）と乾燥ピリジン125 mg（1.60 mmol），乾燥THF（4 mL）を入れた．そこへ，6-(4-cyanobiphenyl-4′-oxy)hexanoyl chloride 526 mg（1.60 mmol）の乾燥THF（3 mL）溶液を氷冷下で滴下した．滴下終了後，50 ℃で3日間加熱かくはんした．反応終了後，水（3 mL）を加えて生成した塩酸塩を溶かし，有機層を分取した．有機層を飽和塩化ナトリウム水溶液（5 mL）で洗浄した後，無水硫酸ナトリウムで乾燥した．溶媒を減圧留去した後，カラムクロマトグラフ（シリカゲル）により粗生成物を得た．溶出物を濃縮後，リサイクル型GPCで分取し，さらに分取TLC（シリカゲル）で精製して白色固体を得た．

収量：82 mg，収率：22%，Rf値：0.34～0.46（展開溶媒　クロロホルム：メタノール＝100：1）

$^1$H NMR($CDCl_3$)：$\delta$ −0.059(s, 3 H, Si$\underline{CH_3}$(G 0))，0.4～0.7(m, 102 H, Si$\underline{CH_2}$(G 0), Si$\underline{CH_2}$(G 2), Si$\underline{CH_2}$(G 1))，1.2～1.4(m, 24 H, SiC$\underline{CH_2}$(G 1), SiC$\underline{CH_2}$(G 0))，1.4～1.5(m, 54 H, C(O)CC$\underline{CH_2}$)，1.5～1.7(m, 102 H, C(O)C$\underline{CH_2}$, SiC$\underline{CH_2}$(G 2))，1.7～1.8(m, 54 H, $\underline{CH_2}$COPh)，2.30(t, 54 H, J=7.48, C(O)$\underline{CH_2}$)，3.9～4.0(m, 54 H, $\underline{CH_2}$OPh)，3.99(t, 54 H, J=6.96, $\underline{CH_2}$OC(O))，6.8～7.0(d, 54 H, phenyl(OCC$\underline{H}$))，7.4～7.5(d, 54 H, phenyl(OCCHC$\underline{H}$))，7.5～7.6(d, 54 H, phenyl(C$\underline{H}$CHCCN))，7.6～7.7(d, 54 H, phenyl(C$\underline{H}$CCN))．

$^{13}$C NMR($CDCl_3$)：$\delta$ 8.02(Si$\underline{CH_2}$(G 2))，17.4(Si$\underline{CH_2}$(G 1))，17.5(Si$\underline{CH_2}$(G 1))，18.5(SiC$\underline{CH_2}$(G 1))，23.2(SiC$\underline{CH_2}$(G 2))，24.7(C(O)C$\underline{CH_2}$)，25.7(C(O)CC$\underline{CH_2}$)，28.9($\underline{CH_2}$COPh)，34.0(C(O)$\underline{CH_2}$)，66.8($\underline{CH_2}$OC(O))，67.8($\underline{CH_2}$OPh)，110.1(phenyl($\underline{C}$CN))，115.0(phenyl(OC$\underline{C}$H))，119.0($\underline{C}$N)，127.0(phenyl($\underline{C}$HCHCCN))，128.3(phenyl(OCCH$\underline{C}$H))，131.4(phenyl(OCCHCH$\underline{C}$))，132.5(phenyl($\underline{C}$HCCN))，145.1(phenyl($\underline{C}$CHCHCCN))，159.6(phenyl(O$\underline{C}$CH))，173.5(O$\underline{C}$(O))．

FAB-MASS：Calcd. for $C_{213}H_{250}O_{27}N_9Si_5$ $[M+H]^+$：3508.81．Found：3508.95．

**3.3.2 Me$_2$G 2-Mesogenの合成** Me$_1$G 2-Mesogenとほぼ同様の方法で白色固体を得た．

収量：181 mg，収率：44%，Rf値：0.37～0.49（展開溶媒　クロロホルム：メタノール＝100：1）

$^1$H NMR($CDCl_3$)：$\delta$ −0.048(s, 6 H, Si$\underline{CH_3}$(G 0))，0.4～0.7(m, 68 H, Si$\underline{CH_2}$(G 0), Si$\underline{CH_2}$(G 2), Si$\underline{CH_2}$(G 1))，1.2～1.4(m, 16 H, SiC$\underline{CH_2}$(G 1), SiC$\underline{CH_2}$(G 0))，1.4～1.5(m, 36 H, C(O)CC$\underline{CH_2}$)，1.5～1.7(m, 72 H, C(O)C$\underline{CH_2}$, SiC$\underline{CH_2}$(G 2))，1.7～1.8(m, 36 H, $\underline{CH_2}$COPh)，2.30(t, 36 H, J=7.48, C(O)$\underline{CH_2}$)，3.9～4.0(m, 36 H, $\underline{CH_2}$OPh)，3.99(t, 36 H, J=6.96, $\underline{CH_2}$OC(O))，6.8～7.0(d, 36 H, phenyl(OCC$\underline{H}$))，7.4～7.5(d, 36 H, phenyl(OCCHC$\underline{H}$))，7.5～7.6(d, 36 H, phenyl(C$\underline{H}$CHCCN))，7.6～7.7(d, 36 H, phenyl(C$\underline{H}$CCN))．

$^{13}$C NMR($CDCl_3$)：$\delta$ −3.51(Si$\underline{CH_3}$(G 0))，7.95(Si$\underline{CH_2}$(G 2))，17.4(Si$\underline{CH_2}$(G 1))，17.6(Si$\underline{CH_2}$(G 1))，18.4(SiC$\underline{CH_2}$(G 1))，23.1(SiC$\underline{CH_2}$(G 2))，24.7(C(O)C$\underline{CH_2}$)，25.7(C(O)CC$\underline{CH_2}$)，28.9($\underline{CH_2}$COPh)，34.0(C(O)$\underline{CH_2}$)，66.8($\underline{CH_2}$OC(O))，67.7($\underline{CH_2}$OPh)，110.1(phenyl($\underline{C}$CN))，115.0(phenyl(OC$\underline{C}$H))，119.0($\underline{C}$N)，127.0(phenyl($\underline{C}$HCHCCN))，128.3(phenyl(OCCH$\underline{C}$H))，131.3(phenyl(OCCHCH$\underline{C}$))，132.5(phenyl($\underline{C}$HCCN))，145.0(phenyl($\underline{C}$CHCHCCN))，159.5(phenyl(O$\underline{C}$CH))，173.4(O$\underline{C}$(O))．

FAB-MASS：Calcd. for $C_{422}H_{487}O_{54}N_{18}Si_9$ $[M+Na]^+$：6950.38．Found：6950.10．

**3.3.3 Me$_3$G 2-Mesogenの合成** Me$_1$G 2-Mesogenとほぼ同様の方法で白色固体を得た．

収量：152 mg，収率：38%，Rf値：0.47～0.60（展開溶媒　クロロホルム：メタノール＝100：1）

$^1$H NMR($CDCl_3$)：$\delta$ −0.034(s, 9 H, Si$\underline{CH_3}$(G 0))，0.4～0.7(m, 34 H, Si$\underline{CH_2}$(G 0), Si$\underline{CH_2}$(G 2), Si$\underline{CH_2}$(G 1))，1.2～1.4(m, 8 H, SiC$\underline{CH_2}$(G 1), SiC$\underline{CH_2}$(G 0))，1.4～1.5(m, 18 H, C(O)CC$\underline{CH_2}$)，1.5～1.7(m, 36 H, C(O)C$\underline{CH_2}$, SiC$\underline{CH_2}$(G 2))，1.7～1.8(m, 18 H, $\underline{CH_2}$COPh)，2.30(t, 18 H, J=7.48, C(O)$\underline{CH_2}$)，3.9～4.0(m, 18 H, $\underline{CH_2}$OPh)，3.99(t, 18 H, J=6.96, $\underline{CH_2}$OC(O))，6.8～7.0(d, 18 H, phenyl(OCC$\underline{H}$))，7.4～7.5(d, 18 H, phenyl(OCCHC$\underline{H}$))，7.5～7.6(d, 18 H, phenyl(C$\underline{H}$CHCCN))，7.6～7.7(d, 18 H, phenyl(C$\underline{H}$CCN))．

$^{13}$C NMR(CDCl$_3$)：$\delta$ −1.46(SiCH$_3$(G 0))，8.02(SiCH$_2$(G 2))，17.3(SiCH$_2$(G 1))，17.8(SiCH$_2$(G 1))，18.4(SiCCH$_2$(G 1))，23.2(SiCCH$_2$(G 2))，24.7(C(O)CCH$_2$)，25.7(C(O)CCCH$_2$)，28.9(CH$_2$COPh)，34.0(C(O)CH$_2$)，66.8(CH$_2$OC(O))，67.8(CH$_2$OPh)，110.1(phenyl(CCN))，115.0(phenyl(OCCH))，119.0(CN)，127.0(phenyl(CHCHCCN))，128.3(phenyl(OCCHCH))，131.3(phenyl(OCCHCHC))，132.5(phenyl(CHCCN))，145.1(phenyl(CCHCHCCN))，159.6(phenyl(OCCH))，173.5(OC(O))．

MALDI/TOF-MASS：Calcd. for $C_{631}H_{723}O_{81}N_{27}Si_{63}$ [M+Na]$^+$57%＋[M+K]$^+$43%：10376.89．Found：10377.61．

**3.3.4 Gradient G 2-Mesogen の合成**

**3.3.4.1 Tetrakis(triallylsilylethyl)silane (1) の合成** アルゴン置換したフラスコにテトラビニルシラン 2.00 g (14.7 mmol)，乾燥 THF (3.4 mL)，speier 触媒のイソプロパノール溶液 4 滴を入れた．そこへトリクロロシラン 11.9 g (88.1 mmol) の乾燥 THF (3.4 mL) 溶液を氷冷下で滴下した．滴下終了後，室温で一晩かくはんし，さらに 2 時間加熱還流させた．次に過剰なトリクロロシランを常圧留去し，残った THF を減圧留去することにより粗クロロシラン誘導体を得た．

別途マグネシウム粉末 11.5 g (473 mmol) と臭化アリル 55.3 g (440 mmol) および乾燥エーテル (200 mL) を用いて，アリルグリニャール試薬を調製した．

先に合成した粗クロロシラン誘導体に乾燥 THF 32 mL を加え，そこにアリルグリニャール試薬を滴下した．滴下終了後 2 時間加熱還流させ，さらにエーテルを常圧留去した後，一晩加熱還流させた．反応終了後，1 N 塩酸水溶液 (84 mL) を加え，有機層を分取し，水 (10 mL) で 2 回，飽和塩化ナトリウム水溶液 (10 mL) で 1 回洗浄した後，無水硫酸ナトリウムを加え乾燥した．溶媒を留去後，カラムクロマトグラフ (シリカゲル) で精製することにより **1** を得た．

収量：6.39 g，収率：58%，Rf 値：0.28～0.43 (展開溶媒　ヘキサン：酢酸エチル＝99：1)

$^1$H NMR(CDCl$_3$)：$\delta$ 0.40～0.45(m, 16 H, SiCH$_2$(G 0))，1.60(d, 24 H, J=8.08 Hz, SiCH$_2$(G 1))，4.8～4.9(m, 24 H, SiCCCH$_2$(G 1))，5.7～5.9(m, 12 H, SiCCH(G 1))．

$^{13}$C NMR(CDCl$_3$)：$\delta$ 2.42(SiCH$_2$(G 0))，3.55(SiCH$_2$(G 0))，19.2(SiCH$_2$(G 1))，114(SiCCCH$_2$(G 1))，134(SiCCH(G 1))．

**3.3.4.2 Tetrakis(tris(triallylsilylpropyl)silylethyl)silane (2) の合成**　アルゴン置換したフラスコに化合物 **1** 2.10 g (2.82 mmol)，乾燥 THF (3.8 mL)，speier 触媒のイソプロパノール溶液 4 滴を入れた．そこへトリクロロシラン 6.87 g (50.7 mmol) の乾燥 THF (3.8 mL) 溶液を氷冷下で滴下した．滴下終了後，室温で一晩かくはんし，さらに 2 時間加熱還流させた．次に過剰なトリクロロシランを常圧留去し，その後残った THF を減圧留去することにより粗クロロシラン誘導体を得た．

別途マグネシウム粉末 6.78 g (278 mmol) と臭化アリル 30.7 g (254 mmol) および乾燥エーテル 100 mL よりアリルグリニャール試薬を調製した．それを先に合成した粗クロロシラン誘導体の乾燥 THF (64 mL) 溶液にゆっくり加えた．滴下終了後，2 時間加熱還流させ，エーテルを常圧留去した後さらに一晩加熱還流させた．反応終了後，常法により処理した．カラムクロマトグラフ(シリカゲル) で精製することにより **2** を得た．

収量：3.74 g，収率：52%，Rf 値：0.22～0.33 (展開溶媒　ヘキサン：酢酸エチル＝99：1)

$^1$H NMR(CDCl$_3$)：$\delta$ 0.3～0.4(m, 16 H, SiCH$_2$(G 0))，0.5～0.7(m, 48 H, SiCH$_2$(G 1))，1.3～1.4(m, 24 H, SiCCH$_2$(G 1))，1.58(d, 72 H, J=8.05 Hz, SiCH$_2$(G 2))，4.8～4.9(m, 72 H, SiCCCH$_2$(G 2))，5.7～5.9(m, 36 H, SiCCH(G 2))．

$^{13}$C NMR(CDCl$_3$)：$\delta$ 3.12(SiCH$_2$(G 0))，5.08(SiCH$_2$(G 0))，16.7(SiCH$_2$(G 1))，17.1(SiCH$_2$(G 1))，18.4(SiCCH$_2$(G 1))，19.7(SiCH$_2$(G 2))，114(SiCCCH$_2$(G 2))，134(SiCCH(G 2))．

**3.3.4.3 Tetrakis(tris(tris(3-hydroxypropyl)silylpropyl)silylethyl)silane (3) の合成**　ボラン THF 錯体の THF 溶液 21.0 mL (21.0 mmol) とシクロヘキセン 3.44 g (42.0 mmol) からジシクロヘキシルボランを調製した．そこに，化合物 **2** 1.00 g (0.389 mmol) の乾燥 THF (10 mL) 溶液を氷冷下で滴下し，滴下終了後，室温で 3 時間かくはんした．さらに，ボラン THF 錯体の THF 溶液 (2.0 mL, 2.0 mmol) を滴下し，室温で 1 時間かくはんした．反応終了後，常法により処理して得た有機層に無水硫酸ナトリウムを加え乾燥した．溶媒を留去後，再沈殿 (メタノール少量に溶かし，ヘキサン：酢酸エチル＝1：1 に滴下) により **3** を得た．

収量：1.19 g，収率：95%

$^1$H NMR(DMSO-d$_6$)：$\delta$ 0.2～0.3(m, 16 H, SiCH$_2$(G 0))，0.4～0.5(m, 72 H, SiCH$_2$(G 2))，0.5～0.6(m, 48 H, SiCH$_2$(G 1))，1.2～1.3(m, 24 H, SiCCH$_2$(G 1))，1.3～1.4(m, 72 H, SiCCH$_2$(G 2))，3.30(q, 72 H, J=5.76 Hz, CH$_2$O)，4.48(t, 36 H, J=5.00 Hz, OH)．

$^{13}$C NMR(DMSO-d$_6$)：$\delta$ 2.53(SiCH$_2$(G 0))，4.91(SiCH$_2$(G 0))，8.22(SiCH$_2$(G 2))，16.9(SiCH$_2$(G 1))，17.4(SiCH$_2$(G 1))，18.5(SiCCH$_2$(G 1))，27.3(SiCCH$_2$(G 2))，64.4(CH$_2$OH)．

**3.3.4.4 Tetrakis(tris(tris(3-methanesulfonylpropyl)silylpropyl)silylethyl)silane (4) の合成**　アルゴン置換したフラスコに化合物 **3** 1.15 g (0.375 mmol)，乾燥ピリジン (8.0 mL) を入れた．塩化メタンスルフォニル 4.42 g (38.5 mmol) を氷冷下で滴下し，滴下終了後，0 ℃ で

2時間かくはんさせた．反応終了後，クロロホルム（10 mL），水（10 mL）の順に氷冷下で滴下した．有機層を分取し，5% 硫酸水溶液で洗浄し，5% 炭酸水素ナトリウム水溶液（5 mL）で2回，飽和塩化ナトリウム水溶液で2回洗浄した後，無水硫酸ナトリウムを加え乾燥した．溶媒を留去した後，カラムクロマトグラフ（シリカゲル）で精製することにより **4** を得た．

収量：1.41 g，収率：66%，Rf値：0.10～0.28（展開溶媒　クロロホルム：メタノール＝20：1）

$^1$H NMR($CDCl_3$)：$\delta$ 0.3～0.4(m, 16 H, $SiCH_2$(G 0))，0.6～0.7(m, 120 H, $SiCH_2$(G 1)，$SiCH_2$(G 2))，1.2～1.4(m, 24 H, $SiCCH_2$(G 1))，1.7～1.8(m, 72 H, $SiCCH_2$(G 2))，3.02(s, 108 H, $SO_2CH_3$)，4.17(t, 72 H, J＝6.50 Hz, $CH_2O$)．

$^{13}$C NMR($CDCl_3$)：$\delta$ 2.90($SiCH_2$(G 0))，5.29($SiCH_2$(G 0))，7.50($SiCH_2$(G 2))，17.1($SiCH_2$(G 1))，18.5($SiCCH_2$(G 1))，23.7($SiCCH_2$(G 2))，37.1($SO_2CH_3$)，72.7($CH_2O$)．

**3.3.4.5　Tetrakis(tris(tris(3-cyanopropyl)silylpropyl)silylethyl)silane (5)** の合成　アルゴン置換したフラスコに化合物 **4** 1.96 g (0.325 mmol)，ヨウ化ナトリウム 78 mg(0.525 mmol)，シアン化ナトリウム 2.29 g(46.8 mol)，乾燥ユーブタノン（50 mL）を入れ，2日間加熱還流させた．反応終了後，水（10 mL），酢酸エチル（10 mL）を加えた．有機層を分取し，水 5 mL で2回，飽和塩化ナトリウム水溶液（5 mL）で3回洗浄した後，無水硫酸ナトリウムを加え乾燥させた．溶媒を留去した後，カラムクロマトグラフ(シリカゲル)で精製して **5** を得た．

収量：1.00 g，収率：87%，Rf値：0.28～0.41（展開溶媒　クロロホルム：メタノール＝20：1）

$^1$H NMR($CDCl_3$)：$\delta$ 0.3～0.5(m, 16 H, $SiCH_2$(G 0))，0.6～0.8(m, 120 H, $SiCH_2$(G 1)，$SiCH_2$(G 2))，1.3～1.5(m, 24 H, $SiCCH_2$(G 1))，1.6～1.8(m, 72 H, $SiCCH_2$(G 2))，2.42(t, 72 H, J＝6.96 Hz, $CH_2CN$)．

$^{13}$C NMR($CDCl_3$)：$\delta$ 2.87($SiCH_2$(G 0))，5.02($SiCH_2$(G 0))，11.5($SiCH_2$(G 2))，16.9($SiCH_2$(G 1))，17.0($SiCH_2$(G 1))，18.4($SiCCH_2$(G 1))，20.3($SiCCH_2$(G 2))，20.8($CH_2CN$(G 2))，120($CN$)．

**3.3.4.6　Tetrakis(tris(tris(3-ethoxycarbonylpropyl)silylpropyl)silylethyl)silane (6)** の合成　フラスコに化合物 **5** 0.41 g (0.112 mmol)，66 wt%硫酸水溶液 (3.9 mL) を入れ，1.5 時間加熱還流させた．次に 99% エタノール (10 mL) を加え一晩かくはんさせた．反応終了後，水 (10 mL)，エーテル（25 mL）を加えた．有機層を分取し，5% 炭酸水素ナトリウム水溶液（5 mL）で3回，飽和塩化ナトリウム水溶液（5 mL）で1回洗浄した後，無水硫酸ナトリウムを加え乾燥した．溶媒を留去した後，カラムクロマトグラフ（シリカゲル）で精製して **6** を得た．

収量：445 mg，収率：74%，Rf値：0.74～0.88（展開溶媒　酢酸エチル）

$^1$H NMR($CDCl_3$)：$\delta$ 0.2～0.4(m, 16 H, $SiCH_2$(G 0))，0.5～0.7(m, 120 H, $SiCH_2$(G 1)，$SiCH_2$(G 2))，1.24(t, 108 H, J＝7.08 Hz, $COOCH_2CH_3$)，1.3～1.4(m, 24 H, $SiCCH_2$(G 1))，1.5～1.7(m, 72 H, $SiCCH_2$(G 2))，2.30(t, 72 H, J＝7.04 Hz, $CH_2COO$)，4.11(q, 72 H, J＝7.00 Hz, $OCH_2$)．

$^{13}$C NMR($CDCl_3$)：$\delta$ 2.93($SiCH_2$(G 0))，5.46($SiCH_2$(G 0))，11.7($COOCH_2CH_3$)，14.2($SiCH_2$(G 2))，17.4($SiCH_2$(G 1))，17.5($SiCH_2$(G 1))，18.7($SiCCH_2$(G 1))，20.9($SiCCH_2$(G 2))，38.0($CH_2COO$)，60.1($COOCH_2$)，173($COOCH_2$)．

**3.3.4.7　Tetrakis(tris(tris(4-hydroxybuthyl)silylpropyl)silylethyl)silane (7 Gradient G 2-OH)** の合成　アルゴン置換したフラスコに水素化リチウムアルミニウム 316 mg (8.33 mmol)，乾燥 THF (18 mL) を入れた．そこへ化合物 **6** 485 mg (0.0925 mmol) の乾燥 THF (12 mL) 溶液を氷冷下で滴下した．滴下終了後，90 ℃ で一晩加熱還流させた．反応終了後，飽和硫酸ナトリウム水溶液 (10 mL) を加えた．遠心分離にかけ，上澄み液を取り出し，飽和塩化ナトリウム水溶液（5 mL）で3回洗浄した後，無水硫酸ナトリウムを加え乾燥した．溶媒を留去後，再沈殿（メタノール少量に溶かしヘキサン：酢酸エチル＝3：1に滴下）により **7** を得た．

収量：291 mg，収率：85%

$^1$H NMR(DMSO-$d_6$)：$\delta$ 0.2～0.4(m, 16 H, $SiCH_2$(G 0))，0.4～0.5(m, 72 H, $SiCH_2$(G 2))，0.5～0.6(m, 48 H, $SiCH_2$(G 1))，1.2～1.3(m, 96 H, $SiCCH_2$(G 1), $SiCCH_2$(G 2))，1.3～1.5(m, 72 H, $SiCCCH_2$(G 2))，3.3～3.4(m, 72 H, $CH_2O$)，4.34(t, 36 H, J＝4.56 Hz, $OH$)．

$^{13}$C NMR(DMSO-$d_6$)：$\delta$ 2.53($SiCH_2$(G 0))，4.75($SiCH_2$(G 0))，12.2($SiCH_2$(G 2))，16.7($SiCH_2$(G 1))，17.3($SiCH_2$(G 1))，18.4($SiCCH_2$(G 1))，20.1($SiCCH_2$(G 2))，36.9($SiCCCH_2$(G 2))，60.7($CH_2OH$)．

**3.3.4.8　Tetrakis(tris(tris(4-(6-(4-cyanobiphenyl-4′-oxy)hexanoyloxy)butyl)silylpropyl)silylethylsilane (Gradient G 2-Mesogen)** の合成　アルゴン置換したフラスコに Gradient G 2-OH 93 mg (0.025 mmol) と乾燥ピリジン 106 mg (1.35 mmol)，乾燥 THF (4 mL) を入れた．そこへ，6-(4-cyanobiphenyl-4′-oxy)hexanoyl chloride 442 mg (1.35 mmol) の乾燥 THF (3 mL) 溶液を氷冷下で滴下し，滴下終了後，50 ℃ で3日間加熱かくはんした．反応終了後，水 (3 mL) を加えて生成した塩酸塩を溶かし，有機層を分取した．有機層を飽和塩化ナトリウム水溶液 (5 mL) で洗浄した後，無水硫酸ナトリウムを加え乾燥した．溶媒を減圧留去した後，カラムクロマトグラフ(シリカゲル)で粗精製物を得，リサイクル型 GPC

で分取し，さらに分取TLC（シリカゲル）で精製して白色固体を得た．

収量：90 mg，収率：25%，Rf値：0.24～0.37(展開溶媒　クロロホルム：メタノール＝100：1)

$^1$H NMR($CDCl_3$)：$\delta$ 0.2～0.4(m, 16 H, $SiCH_2$(G 0))，0.5～0.7(m, 120 H, $SiCH_2$(G 2)，$SiCH_2$(G 1))，1.2～1.4(m, 96 H, $SiCCH_2$(G 1)，$SiCCH_2$(G 2))，1.4～1.5(m, 72 H, $C(O)CCCH_2$)，1.6～1.7(m, 144 H, $CH_2COC(O)$，$C(O)CCH_2$)，1.7～1.8(m, 72 H, $CH_2COPh$)，2.30(t, 72 H, J=7.40, $C(O)CH_2$)，3.9～4.0(m, 72 H, $CH_2OPh$)，4.05(t, 72 H, J=6.68, $CH_2OC(O)$)，6.8～7.0(d, 72 H, phenyl(OCCH))，7.4～7.5(d, 72 H, phenyl(OCCHCH))，7.5～7.6(d, 72 H, phenyl(CHCHCCN))，7.54(d, 72 H, J=3.54 Hz, phenyl(CHCCN))．

$^{13}$C NMR($CDCl_3$)：$\delta$ 2.99($SiCH_2$(G 0))，5.62($SiCH_2$(G 0))，12.0($SiCH_2$(G 2))，17.5($SiCH_2$(G 1))，18.0($SiCH_2$(G 1))，18.8($SiCCH_2$(G 1))，20.3($SiCCH_2$(G 2))，24.7($SiCCCH_2$(G 2))，25.7($C(O)CCCH_2$)，28.9($CH_2COPh$)，32.6($C(O)CCH_2$)，34.0($C(O)CH_2$)，63.7($CH_2OC(O)$)，67.6($CH_2OPh$)，110.1(phenyl(CCN))，114.9(phenyl(OCCH))，118.8(CN)，126.8(phenyl(CHCHCCN))，128.2(phenyl(OCCHCH))，131.3(phenyl(OCCHCHC))，132.5(phenyl(CHCCN))，144.8(phenyl(CCHCHCCN))，159.4(phenyl(OCCH))，173.3($OC(O)$)．

MALDI/TOF-MASS：Calcd. for $C_{872}H_{1024}O_{108}N_{36}Si_{17}$ [M+Na]$^+$44%＋[M+K]$^+$56%：14247.43. Found：14252.72.

## 文　献


1) a) F. Zeng and S. C. Zimmerman, *Chem. Rev.*, **97**, 1681 (1997); b) A. W. Bosman, H. M. Janssen, and E. W. Meijer, *Chem. Rev.*, **99**, 1665 (1999); c) D. Astruc and F. Chardac, *Chem. Rev.*, **101**, 2991 (2001).

2) a) A. W. Made and P. W. N. Leeuwen, *J. Chem. Soc., Chem. Commun.*, 1400 (1992); b) H. Frey, C. Lach, and K. Lorenz, *Adv. Mater.*, **10** (4), 279 (1998); c) J. P. Majoral and A. M. Caminade, *Chem. Rev.*, **99**, 845 (1999).

3) L. L. ZouhL and J. Roovers, *Macromolecules*, **26**, 963 (1993).

4) K. Lorenz, D. Holter, B. Stuhn, R. Mulhhaupt, and H. Frey, *Adv. Mater.*, **8** (5), 414 (1996).

5) a) D. Terunuma, T. Kato, R. Nishio, K. Matsuoka, H. Kuzuhara, Y. Aoki, and H. Nohira, *Chem. Lett.*, **1998**, 59; b) D. Terunuma, T. Kato, R. Nishio, Y. Aoki, H. Nohira, K. Matsuoka, and H. Kuzuhara, *Bull. Chem. Soc. Jpn.*, **72**, 2129 (1999).


**Preparation of New Carbosilane Dendrimers Having Terminal Mesogens and Investigation of Their Liquid Crystal Characteristics**


Takaki TSUCHIDA,*1 Chiemi SHIMAZAKI,*1 Ken HATANO,*1 Koji MATSUOKA,*1 Yoshio AOKI,*1 Hiroyuki NOHIRA,*1 Yasuaki ESUMI,*2 and Daiyo TERUNUMA*1

*1*Department of Functional Materials Science, Faculty of Engineering, Saitama University (Shimo-Ohkubo, Sakura-ku, Saitama-shi, Saitama 338-8570, Japan)*

*2*The Institute of Physical and Chemical Research (RIKEN) (Wako-shi, Saitama 351-0198, Japan)*



Both of a series of new second generation carbosilane dendrimers having a different number of branches ($Me_nG$ 2-Mesogen, n=1, 2, 3) and a novel carbosilane dendrimer having an increased length of methylene chain from the core to the second generation (Gradient G 2-Mesogen) with terminal cyanobiphenyl mesogens were prepared. The characterization of the dendrimers was carried out by using differential scanning calorimetry (DSC) and optical polarizing microscopy. All the dendrimers showed smectic A phase. The ranges of the smectic A phase and the texture size of $Me_nG$ 2-Mesogen were increased with increasing the number of branches. The behavior of phase transition temperature and the texture size of Gradient G 2-Mesogen were similar to those of $Me_0G$-2 Mesogen.



KEY WORDS　Carbosilane Dendrimer / Synthesis / Liquid Crystal / Cyanobiphenyl /

(Received May 16, 2003: Accepted July 17, 2003)　[*Kobunshi Ronbunshu*, **60**(10), 561—568 (2003)]

# A therapeutic agent with oriented carbohydrates for treatment of infections by Shiga toxin-producing *Escherichia coli* O157:H7

Kiyotaka Nishikawa*†, Koji Matsuoka‡, Eiji Kita§, Noriko Okabe*, Masashi Mizuguchi¶, Kumiko Hino*, Shinobu Miyazawa*, Chisato Yamasaki*, Junken Aoki‖, Sachio Takashima**, Yoshio Yamakawa††, Masahiro Nishijima††, Daiyo Terunuma‡, Hiroyoshi Kuzuhara‡, and Yasuhiro Natori*

*Department of Clinical Pharmacology, Research Institute, International Medical Center of Japan, 1-21-1 Toyama, Shinjuku-ku, Tokyo 162-8655, Japan; ‡Department of Functional Materials Science, Saitama University, 255 Shimookubo, Urawa-shi, Saitama 338-8570, Japan; §Department of Bacteriology, Nara Medical University, Kashihara, Nara 634-8521, Japan; ¶Department of Pediatrics, Jichi Medical School, 3311-1 Yakushiji, Minamikawachi-machi, Kawachi-gun, Tochigi 329-0498, Japan; ‖Department of Health Chemistry, Faculty of Pharmaceutical Sciences, University of Tokyo, 7-3-1 Hongo, Bunkyo-ku, Tokyo 113-0033, Japan; **National Institute of Neuroscience, 4-1-1 Okawahigashi-machi, Kodaira-shi, Tokyo 187-8502, Japan; and ††Division of Biochemistry and Cell Biology, National Institute of Infectious Diseases, 1-23-1 Toyama, Shinjuku-ku, Tokyo 162-8640, Japan

Edited by John J. Mekalanos, Harvard Medical School, Boston, MA, and approved April 4, 2002 (received for review February 1, 2002)

**Infection with Shiga toxin (Stx)-producing *Escherichia coli* O157:H7, which causes diarrhea and hemorrhagic colitis in humans, often results in fatal systemic complications, such as neurological damage and hemolytic–uremic syndrome. Because Stx circulating in the blood is a major causative factor of these complications, the development of a Stx neutralizer that functions in the circulation holds promise as a viable therapy. Here we developed a series of carbosilane dendrimers, in which trisaccharides of globotriaosyl ceramide, a receptor for Stx, were variously oriented at their termini (referred to as SUPER TWIG), and identified a SUPER TWIG with six trisaccharides as a Stx neutralizer functioning in the circulation. This SUPER TWIG specifically bound to Stx with high affinity ($K_d$ = 1.1 × $10^{-6}$ M) and inhibited the incorporation of the toxin into target cells. Intravenous administration of the SUPER TWIG along with Stx to mice substantially reduced the fatal brain damage and completely suppressed the lethal effect of Stx. Moreover, the SUPER TWIG protected mice from challenge with a fatal dose of *E. coli* O157:H7, even when administered after the establishment of the infection. The SUPER TWIG neutralized Stx *in vivo* by a mechanism in which the accumulation and immediate degradation of Stx by phagocytic macrophages present in the reticuloendothelial system were induced. Taken together, our findings indicate that this SUPER TWIG is therapeutic agent against infections by Stx-producing *E. coli*.**

Shiga toxin (Stx)-producing *Escherichia coli* (STEC), including O157:H7, causes diarrhea and hemorrhagic colitis in humans. These gastrointestinal diseases are often complicated by potentially fatal systemic sequelae such as neurological damage and hemolytic–uremic syndrome, the leading cause of acute renal failure in children (1–4). Stx produced by STEC in the gut traverses the epithelium and passes into the circulation, where it causes vascular damage in specific target tissues such as brain and kidney, resulting in systemic complications. Therefore, research leading to the development of an effective Stx neutralizer that specifically binds to and inhibits Stx in the circulation would thus be a promising approach as a viable therapy.

Stx, which is classified into two closely related subgroups, Stx1 and Stx2, consists of a catalytic A subunit, which has RNA *N*-glycosidase activity and inhibits eukaryotic protein synthesis, and a pentameric B subunit, which is responsible for binding to the functional cell-surface receptor, globotriaosyl ceramide [$Gb_3$; Galα(1–4)-Galβ(1–4)-Glcβ1-ceramide] (4–6). Highly selective and potent binding of Stx to $Gb_3$ is mainly attributed to the multiple interaction of the B subunit pentamer with the trisaccharide moiety of $Gb_3$. On the basis of these facts, several Stx neutralizers, in which the trisaccharide moiety of $Gb_3$ is combined with various core structures in multiple ways, have been reported (7–10). However, no Stx neutralizer has been developed that is capable of detoxifying the toxin present in the circulation.

In this study, we used a series of carbosilane dendrimers carrying various numbers of the trisaccharide [referred to as SUPER TWIG (11)] to develop a Stx neutralizer that functions in the circulation, because SUPER TWIGs are unique in that the number of the terminal trisaccharides can be easily changed by regulating the number of silicon atoms present in the core structure and the silicon–carbon bond is generally biologically inert. We found that SUPER TWIG with six trisaccharides effectively neutralized Stx in the circulation. Furthermore, the SUPER TWIG protected mice from challenge with a fatal dose of STEC O157:H7, suggesting that the SUPER TWIG can be a practical therapeutic agent against infections by STEC.

## Materials and Methods

**Materials.** SUPER TWIGs were synthesized as described (11), and were characterized by NMR and fast-atom bombardment mass spectrometry to confirm their structures. Recombinant Stx1 and -2 were prepared according to published methods (12). Recombinant glutathione *S*-transferase (GST)-fused Stx1, in which the catalytic A1 subunit of the holotoxin was replaced with GST (referred to as Stx1-A2$B_5$-GST), was prepared as follows. From the pUC118 vector containing the complete coding sequence of Stx1 (construct kindly provided by S. Yamasaki, International Medical Center of Japan, Tokyo) (13), a *Bam*HI–*Eco*RI fragment was prepared by PCR with the following primers: 5′-AGAGGGATCCTCGCGAGTTGCCAGAATG-3′ and 5′-AGAGGAATTCTCAACGAAAAATAACTTCGC-3′. The fragment obtained was ligated into the *Bam*HI–*Eco*RI site of the pGEX-2T vector (Amersham Pharmacia). Competent MC1061 *E. coli* cells (kindly provided by S. Yamasaki) were then transformed with this vector, and the resulting isolated plasmid was designated pStx1-A2$B_5$-GST. pStx1-A2$B_5$-GST-transformed MC1061 *E. coli* cells were cultured in 1 liter of Luria–Bertani broth (Difco) supplemented with 100 μg/ml ampicillin (Meiji Seika, Tokyo) at 30°C to midexponential phase. The culture was subsequently treated with 0.5 mM isopropyl β-D(−)-thiogalactopyranoside (Wako Pure Industries, Osaka) for 4 h at 30°C. Collected cell pellets were lysed in 10 ml of PBS containing 6,000 units/ml polymyxin B (Sigma). After centrifugation, the resulting supernatants were incubated with 50 μl of glutathione-Sepharose beads (Amersham Pharmacia) for 2 h at 4°C. After extensive washing of the beads, soluble Stx1-A2$B_5$-GST

This paper was submitted directly (Track II) to the PNAS office.

Abbreviations: Stx, Shiga toxin; STEC, Shiga toxin-producing *Escherichia coli*; $Gb_3$, globotriaosyl ceramide; GST, glutathione *S*-transferase; TCA, trichloroacetic acid.

†To whom reprint requests should be addressed. E-mail: knishika@ri.imcj.go.jp.

was eluted from the beads by incubating them with elution buffer [75 mM Hepes (pH 7.5)/150 mM NaCl/5 mM DTT/100 mM glutathione; Sigma] for 30 min at 25°C. Hybridoma-13C4, which produces a monoclonal antibody against the Stx1 B subunit, was obtained from the American Type Culture Collection. $^{125}$I-labeled Stx1 ($^{125}$I-Stx1) and Stx2 ($^{125}$I-Stx2) were prepared by the iodine monochloride method as described (14).

**Cells.** Vero cells were maintained in DMEM supplemented with 10% FCS in a 24-well (for binding assay) or 96-well (for cytotoxicity assay) plastic microplate. Mouse peritoneal macrophages were prepared as described (15).

**TLC Immunostaining Assay.** The assay for Stx binding to $Gb_3$ was performed as described (16). Porcine erythrocyte $Gb_3$ (500 ng; Wako Pure Industries) was applied to an HPTLC plate (Whatman) and developed in chloroform/methanol/water (60:35:8, vol/vol). After having been blocked with 1% BSA, the plate was incubated with Stx1 (100 ng/ml) in the presence of the desired amount of a given SUPER TWIG. After extensive washing, monoclonal antibody 13C4 was used for the detection of bound Stx1.

**Kinetic Analysis of SUPER TWIG Binding to Immobilized Stx1-A2B$_5$-GST.** SUPER TWIG binding to immobilized Stx1-A2B$_5$-GST was quantified by using a BIAcore system instrument (Pharmacia Biosensor, Uppsala, Sweden) (17). Goat anti-GST antibody was immobilized on a CM5 sensor chip. Recombinant GST or Stx1-A2B$_5$-GST (10 $\mu$g/ml) was injected into the system to become immobilized on the chip. Various concentrations of SUPER TWIGs were injected (time 0) over the immobilized GST or Stx1-A2B$_5$-GST at a flow rate of 20 $\mu$l/ml for at least 8 min to reach plateau at 25°C. The resonance unit is an arbitrary unit used by the BIAcore system. The resonance unit value obtained from immobilized GST was subtracted from the data obtained from immobilized Stx1-A2B$_5$-GST to correct for the background. The binding kinetics were analyzed by Scatchard plot by using the software BIAEVALUATION 3.0.

**$^{125}$I-Stx-Binding Assay.** Vero cells were treated with $^{125}$I-Stx1 or $^{125}$I-Stx2 ($7 \times 10^6$ cpm/$\mu$g or $2 \times 10^6$ cpm/$\mu$g of protein, respectively; 1 $\mu$g/ml) in the absence or presence of the desired amount of a given SUPER TWIG or with unlabeled Stx1 or Stx2 (50 $\mu$g/ml) for 30 min at 4°C. After extensive washing, the cells were dissolved in lysis solution (0.1 M NaOH/0.5% SDS). Recovered radioactivity was measured by a $\gamma$-counter (Packard). Specific binding of these radiolabeled Stxs was confirmed by the complete inhibition by unlabeled Stxs (data not shown).

**Cytotoxicity Assay.** Subconfluent Vero cells in a 96-well plate were treated with Stx1 or Stx2 (10 pg/ml) in the absence or presence of the desired amount of a given SUPER TWIG for 72 h. Relative cell number was determined by using a WST-1 Cell Counting Kit (Wako Pure Industries).

**Intravenous Administration of Stx2 to Mice.** A lethal dose of Stx2 (0.25 ng/g of body weight) was administered to 14–30 female ICR mice (18–20 g, Japan SLC, Shizuoka, Japan) through a tail vein with or without the desired amount of a given SUPER TWIG, and the survival periods of the mice were monitored. The data were analyzed by Kaplan–Meier survival analysis or, when no mice had died by the end of the observation, by Fisher's exact test. For determining the tissue distribution of Stx2, $^{125}$I-Stx2 ($5 \times 10^6$ cpm/$\mu$g of protein, 0.25 ng/g of body weight) was administered as described above. After 1 h all mice were killed, and the radioactivity present in individual tissues was measured with a $\gamma$-counter. Pieces of the liver were fixed in 10% formalin and used for immunohistochemical examination (see below).

**Histology and Immunohistochemistry.** For histologic and immunohistochemical examination of the brain, five mice were injected intravenously with Stx2 (0.25 ng/g of body weight) alone or Stx2 plus SUPER TWIG (1)6 (15 $\mu$g/g of body weight). After 48 h the mice were killed, and their brains were immediately fixed in 10% formalin. For histologic examination, some of the paraffin-embedded sections were stained with hematoxylin and eosin; and others, with luxol fast blue and cresyl violet. Immunohistologic localization of Stx2 was detected by a rabbit polyclonal antibody against Stx2, as described (18).

**Mouse Infection Protocol.** Specific pathogen-free, 3-week-old female C57BL/6 mice that had been weaned were purchased from Charles River Breeding Laboratories. Animals were fed a low-protein diet (5% protein, wt/wt) for 2 weeks to achieve protein calorie malnutrition (19). Mice at 5 weeks of age were infected intragastrically with $2 \times 10^6$ colony-forming units of *E. coli* O157:H7 strain N-9 as described (19). Mice were fed the low-protein diet even after the

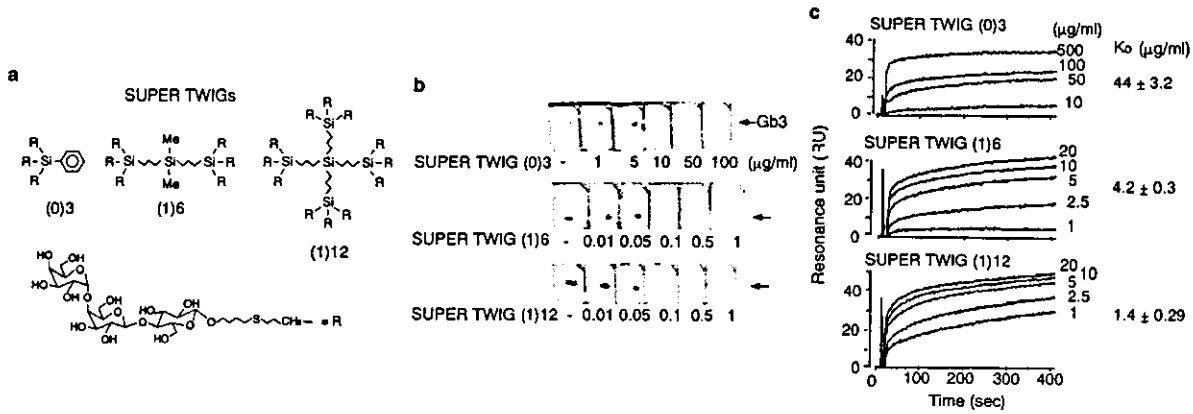


**Fig. 1.** Structures of SUPER TWIGs and their direct binding to Stx. (a) Structures of SUPER TWIG (0)3 ($M_r$ = 2,006; trisaccharide = $1.50 \times 10^{-3}$ mol/g), (1)6 ($M_r$ = 4,001; trisaccharide = $1.50 \times 10^{-3}$ mol/g), and (1)12 ($M_r$ = 7,913; trisaccharide = $1.52 \times 10^{-3}$ mol/g), carrying 3, 6, and 12 trisaccharides of $Gb_3$, respectively. The numbers in parentheses indicate the generation numbers of the SUPER TWIGs. The zero and the first generation of the SUPER TWIGs have one and three linear silicon atoms, respectively, in their core structures. (*b*) TLC immunostaining assay. Double bands were detected, and both were confirmed to be $Gb_3$ by anti-$Gb_3$ staining (data not shown). The data are representative of three experiments. (c) Kinetic analysis of SUPER TWIG binding to immobilized Stx1-A2B$_5$-GST by using the BIAcore system. The binding kinetics were analyzed by Scatchard plot to determine $K_d$ and maximum binding values (means ± SE, $n$ = 5). The maximum binding values of SUPER TWIG (0)3, (1)6, and (1)12 were 43 ± 2.9, 63 ± 2.6, and 57 ± 2.0 resonance units (RU), respectively.

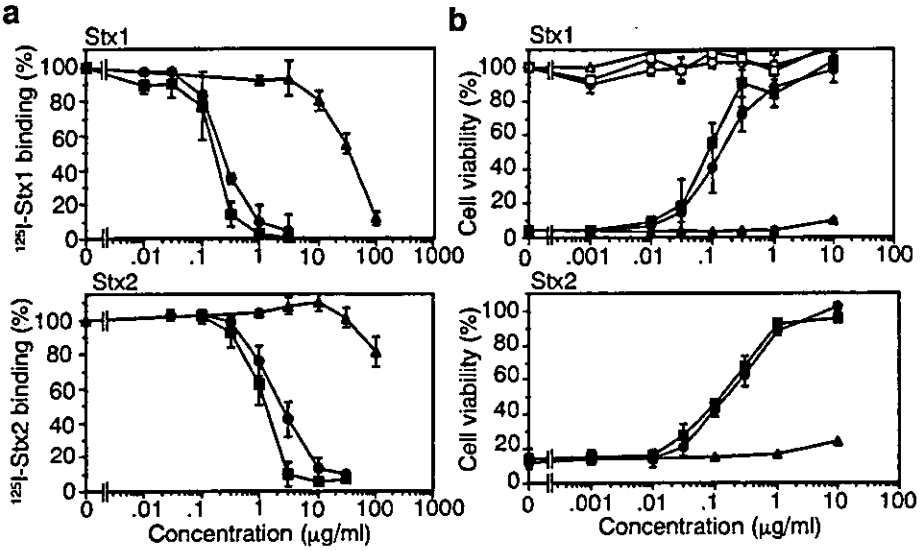


**Fig. 2.** Inhibitory effect of SUPER TWIGs on the biological activities of Stx1 (*Upper*) and Stx2 (*Lower*) in Vero cells. (*a*) $^{125}$I-Stx-binding assays. ▲, ●, and ■ indicate SUPER TWIG (0)3, (1)6, and (1)12, respectively. The data are presented as the percentage of the activity in the absence of SUPER TWIGs (means ± SE, $n$ = 3). (*b*) Cytotoxicity assay with Vero cells. Open symbols indicate SUPER TWIGs only. The data are presented as the percentage of the value in the absence of Stxs (means ± SE, $n$ = 3).

start of the infection. Seven infected mice were given intravenously SUPER TWIG (1)6 (50 μg/g of body weight) dissolved in 0.1 ml of saline twice a day; this treatment was initiated on day 3 of infection and continued until day 6. Ten infected mice were treated with 0.1 ml of saline as a vehicle control by using the same protocol as used for the treatment with SUPER TWIG (1)6. Statistical analysis was performed as described above.

**Metabolism of $^{125}$I-Stx2 in Cells.** Mouse peritoneal macrophages and Vero cells were incubated with $^{125}$I-Stx2 ($2 \times 10^6$ cpm/μg of protein, 1 μg/ml) in the absence or presence of SUPER TWIG (1)6 (10 μg/ml) or a 100-fold excess of nonradioactive Stx2 for the desired periods at 37°C. After extensive washing, cell lysates were separated by electrophoresis on an SDS/15% polyacrylamide gel and visualized by autoradiography. For the degradation experiment of Stx2, macrophages were incubated with $^{125}$I-Stx2 ($2 \times 10^6$ cpm/μg of protein, 1 μg/ml) in the presence of SUPER TWIG (1)6 (10 μg/ml) for 4 h at 37°C. After extensive washing, the culture medium was changed to DMEM without FCS. After the desired periods, the cells were dissolved in lysis solution for SDS/PAGE. The culture medium was recovered, and 100% ice-cold trichloroacetic acid (TCA) was added to a final concentration of 10%. After centrifugation, the precipitated proteins were dissolved in lysis solution for SDS/PAGE. Radioactivity present in each band was quantified by using a bio-imaging analyzer BAS-1000 (Fuji). Radioactivity present in the TCA-soluble supernatants was measured with a γ-counter.

**Uptake of $^{125}$I-Stx2 by Macrophages.** Mouse peritoneal macrophages were incubated with $^{125}$I-Stx2 ($2 \times 10^6$ cpm/μg of protein, 1 μg/ml) in the absence or presence of the desired amount of a given SUPER TWIG for 30 min at 37°C. After extensive washing, the cells were dissolved in lysis solution. Recovered radioactivity was measured by a γ-counter.

## Results and Discussion

**SUPER TWIGs (1)6 and (1)12 Directly Bind to the Stx B Subunit with High Affinity.** Earlier we had developed three SUPER TWIGs, i.e., SUPER TWIG (0)3, (1)6, and (1)12, carrying 3, 6, and 12 trisaccharides, respectively (11) (Fig. 1*a*). These SUPER TWIGs have different numbers of the trisaccharides, but the molar content of trisaccharide per weight is almost the same (see the legend for Fig. 1*a*). Therefore, the concentration of each SUPER TWIG was given as micrograms per milliliter, which enables direct comparison of their activities on a per-trisaccharide basis. Among the SUPER TWIGs, SUPER TWIGs (1)6 and (1)12 at the concentration of 0.5 and 0.1 μg/ml, respectively, completely inhibited the Stx1 binding to $Gb_3$ developed on a TLC plate, both of which concentrations were much lower than the effective concentration observed for SUPER TWIG (0)3 (Fig. 1*b*). With Stx1-A2B$_5$-GST immobilized on a BIAcore sensor chip, the dissociation constant ($K_d$) of each SUPER TWIG to the B subunit pentamer was determined by Scatchard plot analysis. SUPER TWIGs (1)6 and (1)12 showed very low $K_d$ values of 4.2 and 1.4 μg/ml, respectively; whereas the $K_d$ value of SUPER TWIG (0)3 was 30 times higher (44 μg/ml) than that of SUPER TWIG (1)12 (Fig. 1*c*). These results indicate that SUPER TWIGs (1)6 and (1)12 directly bind to the Stx B subunit with high affinity and that six trisaccharides in one molecule are sufficient for the high-affinity binding. Because the terminal trisaccharides of SUPER TWIGs (1)6 and (1)12 were designed to span ≈30 Å from the central silicon atom, which fully embraces the predicted $Gb_3$-binding sites on the B subunit pentamer [both sites 1 and 2 (20)], it is possible that these SUPER TWIGs, but not SUPER TWIG (0)3, effectively occupied the multiple binding sites, resulting in a marked increase in their affinity for the B subunit pentamer. We have already synthesized SUPER TWIGs (1)9, (2)18, and (2)36, carrying 9, 18, and 36 trisaccharides in which all of the —R residues present in SUPER TWIGs (0)3, (1)6, and (1)12, respectively, were replaced with —$(CH_2)_3$—$SiR_3$. These SUPER TWIGs had $K_d$ values similar to the B subunit pentamer (1.7, 1.5, and 1.8 μg/ml, respectively; K.N., K.M., K.H., D.T., H.K., and Y.N., unpublished data), further confirming that at least six trisaccharides with appropriate distance in the molecule are sufficient for the high-affinity binding to the B subunit pentamer.

**Marked Inhibition of the Biological Activities of Stx by SUPER TWIGs (1)6 and (1)12.** SUPER TWIGs (1)6 and (1)12 markedly inhibited the binding of $^{125}$I-labeled Stx1 ($^{125}$I-Stx1) and Stx2 ($^{125}$I-Stx2) to Vero cells, one of the cell types most sensitive to Stx. The half-maximal inhibitory concentrations ($IC_{50}$) of SUPER TWIGs (1)6 and (1)12 for $^{125}$I-Stx1 binding were 0.22 and 0.16 μg/ml, respectively; and those for $^{125}$I-Stx2 were 2.3 and 1.3 μg/ml, respectively (Fig. 2*a*). The $IC_{50}$ value of SUPER TWIG (0)3 for $^{125}$I-Stx1 was 270 times higher than that of SUPER TWIG (1)12, and the $IC_{50}$ value for $^{125}$I-Stx2 was more than 100 μg/ml (Fig. 2*a*). SUPER TWIGs (1)6 and (1)12 markedly inhibited the cytotoxic activity of both Stx1 ($IC_{50}$ = 0.12 and 0.20 μg/ml, respectively) and Stx2 ($IC_{50}$ = 0.17 and 0.23 μg/ml, respectively) toward Vero cells (Fig. 2*b*). In contrast, no inhibitory effect was observed with SUPER TWIG (0)3. Each SUPER TWIG itself did not affect the cell

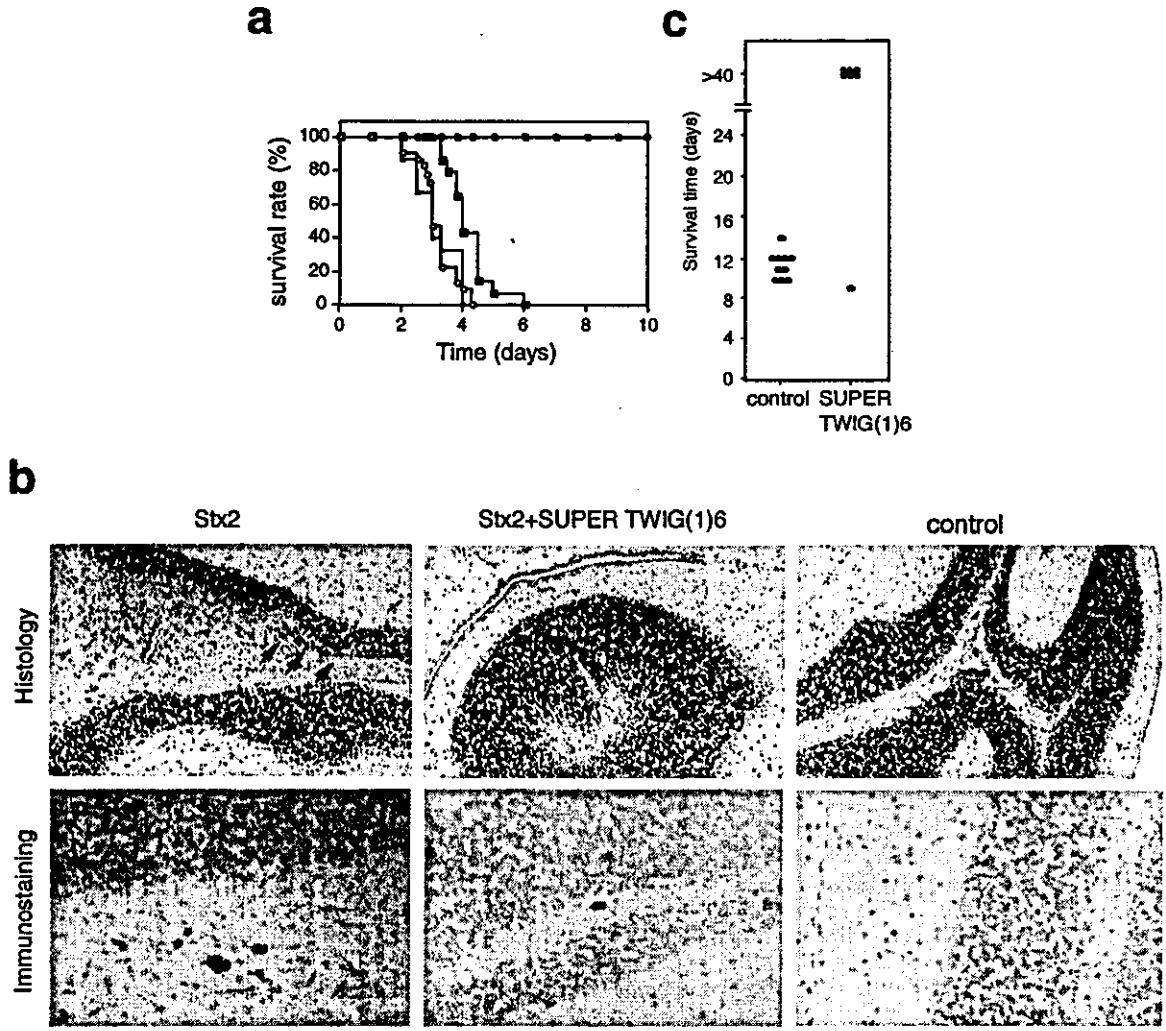


**Fig. 3.** Inhibitory effect of SUPER TWIG (1)6 on the lethality of Stx2 or infection with *E. coli* O157:H7 in mice. (*a*) A lethal dose of Stx2 (0.25 ng/g of body weight) was administered to mice without any SUPER TWIG (○; number of mice = 30) or with SUPER TWIG (0)3 (▲; number of mice = 15), (1)6 (●; number of mice = 20), or (1)12 (▲; number of mice = 14) (50 μg/g of body weight). Data represent the survival rate of each group. Data of the first 10 days are shown. (*b*) Histologic examination and immunostaining of Stx2 in the brain. Sections of cerebellar cortex were used for staining. For histologic examination, the sections were stained with hematoxylin and eosin (*Upper*). Black and yellow arrowheads indicate perivascular hemorrhage and congestion, respectively. Stx2 present in the sections was detected by using specific antibody against Stx2 (*Lower*). (×80.) (*c*) Mice with protein calorie malnutrition were infected intragastrically with *E. coli* O157:H7 strain N-9 ($2 \times 10^6$ colony-forming units) on day 0. SUPER TWIG (1)6 (50 μg/g of body weight) or saline alone was administered intravenously to the mice (control, $n = 10$; SUPER TWIG-treated, $n = 7$) twice a day from day 3 to day 6. Data represent the survival time of each mouse.

viability. These results indicate that SUPER TWIGs (1)6 and (1)12 markedly inhibited the binding of Stx to the functional cell-surface receptor $Gb_3$ on the target cells, consistent with the direct and high-affinity binding of these SUPER TWIGs to the Stx B subunit as described above.

**Effect of SUPER TWIGs *in Vivo*.** Next, we investigated the inhibitory effects of SUPER TWIGs on the lethality of intravenously administered Stx2 in mice. Stx2 was used in this study because Stx2 is more toxic than Stx1 both *in vitro* and *in vivo*, and clinically more significant (6, 21). SUPER TWIG (1)6 completely suppressed the lethal effect of Stx2 when administered along with the toxin; otherwise 100% of the mice died within 5 days (average survival period of mice not given SUPER TWIG (1)6 was 3.2 ± 0.1 days, $P < 0.0001$; Fig. 3*a*). The SUPER TWIG (1)6-treated mice survived more than 2 months without any pathological symptoms (data not shown). The dose of SUPER TWIG (1)6 required for the complete suppression could be reduced to 5.0 μg/g of body weight (data not shown). SUPER TWIG (1)12 lengthened the survival period (average survival period was 4.2 ± 0.2 days, $P < 0.0001$), but none of the SUPER TWIG (1)12-treated mice survived more than 7 days (Fig. 3*a*). No inhibitory effect was observed with SUPER TWIG (0)3. Each SUPER TWIG itself did not affect the viability (data not shown). Considering the observation that SUPER TWIG (1)12 inhibited Stx more effectively than SUPER TWIG (1)6 *in vitro* (Fig. 2), these results suggest that some other factor(s), in addition to the high-affinity binding to Stx, might be involved in the potent Stx-neutralizing activity of SUPER TWIG (1)6 *in vivo*.

Stx2 causes multifocal vascular damage in the central nervous system, which is closely related to its morbidity and mortality in animal models (3, 18, 19, 22–24). Therefore, pathological changes in cerebral blood vessels, such as congestion and hemorrhage, were investigated after the i.v. administration of mice with Stx2 with or without SUPER TWIG (1)6. Forty-eight hours after the injection of Stx2 alone, congestion was noted in all these brains, most commonly in the cerebellum (Fig. 3*b*) and hippocampus (data not

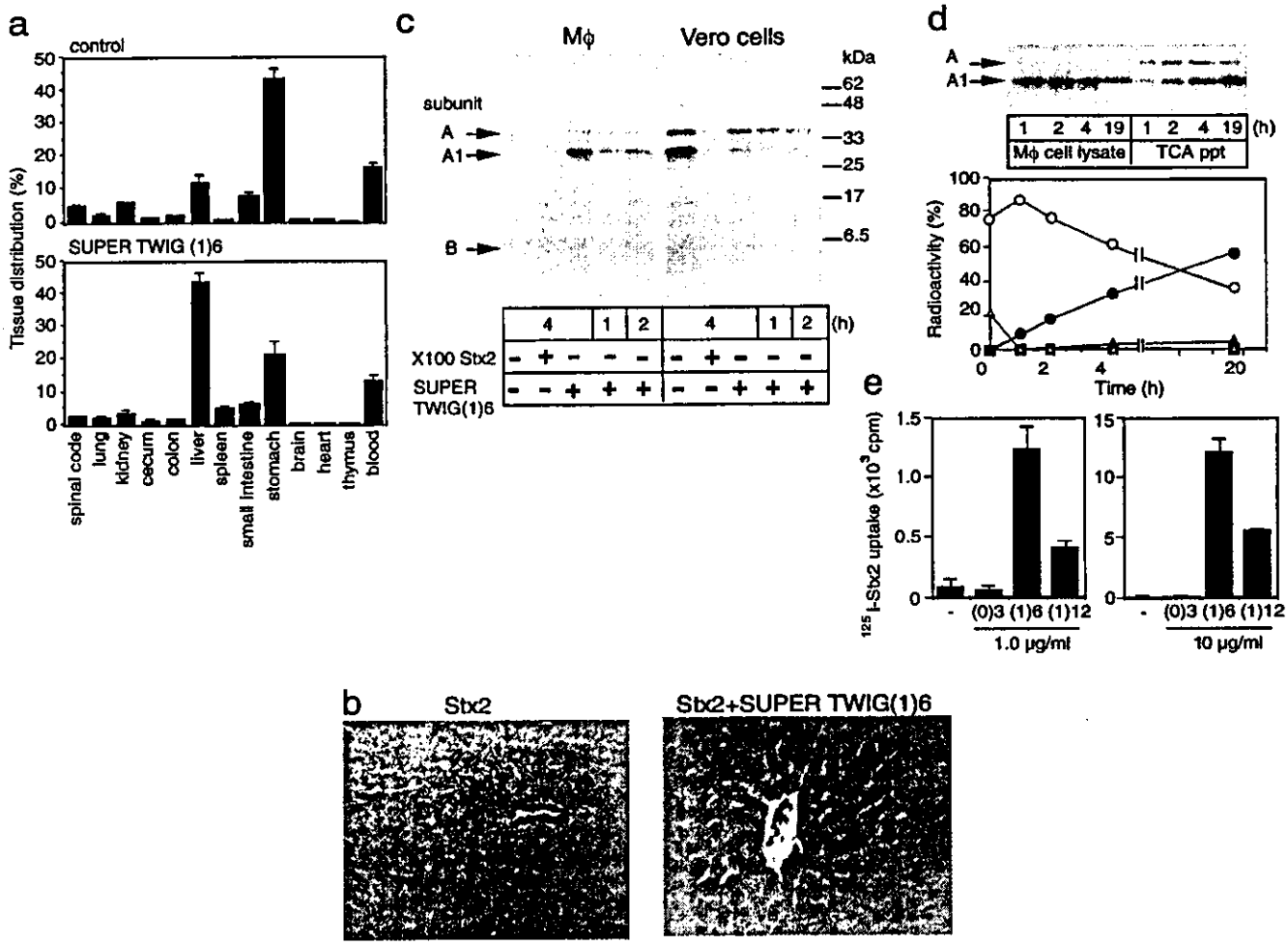


Fig. 4. SUPER TWIG (1)6-dependent degradation of Stx2 in macrophages. (*a*) Tissue distribution of $^{125}$I-Stx2. The data are presented as the percentage of the total radioactivity present in all of the tissues examined (means ± SE, $n = 3$). Total radioactivities for control and SUPER TWIG (1)6-coinjected mice were 8,900 ± 400 and 12,200 ± 2,200 cpm (means ± SE, $n = 3$), respectively. (*b*) Immunostaining of Stx2 in the liver. Stx2 present in the sections was detected by using specific antibody against Stx2. (*c*) Metabolism of $^{125}$I-Stx2 in cells. Mouse peritoneal macrophages (Mϕ) or Vero cells were incubated with $^{125}$I-Stx2 (1 μg/ml) in the absence or presence of SUPER TWIG (1)6 (10 μg/ml) or a 100-fold excess of nonradioactive Stx2 for the indicated periods at 37°C. These lysates were separated by electrophoresis on SDS/15% polyacrylamide gel and bands visualized by autoradiography. (*d*) Degradation of Stx2 in macrophages. Open triangle and open circle indicate A subunit and A1 fragment, respectively, present in the macrophage cell lysate. Filled square and filled triangle indicate A subunit and A1 fragment, respectively, present in the TCA precipitate (ppt) of the culture medium. Because of the low protein content in the TCA ppt fraction, an 8 times larger aliquot of it was used for SDS/PAGE than the amount of the macrophage cell lysate used. Filled circles indicate TCA-soluble supernatants. The data are presented as the percentage of the total radioactivity present in the cell lysate and the culture medium. (e) Effect of SUPER TWIGs on the uptake of $^{125}$I-Stx2 by macrophages. Mouse peritoneal macrophages were incubated with $^{125}$I-Stx2 (1 μg/ml) in the absence or presence of SUPER TWIG (0)3, (1)6, or (1)12 (1 or 10 μg/ml) for 30 min at 37°C. The data are presented as the total radioactivity (cpm) present in the cell lysate (means ± SE, $n = 3$).

shown) compared with the brains of normal mice. Multiple parenchymal microhemorrhage was most frequently observed in the cerebellum, whereas neurons and glial cells seemed to be normal. Stx2 was detected by immunohistochemical examination in red blood cells and vascular endothelium in the cerebellum (Fig. 3*b*), midbrain, and thalamus (data not shown). Neurons, glial cells, and other parenchymal components were negative for Stx2. On the contrary, in SUPER TWIG (1)6-coinjected mice, vascular damage was minimal, where congestion was slight and parenchymal hemorrhage was absent. Concomitantly, Stx2 deposition in the blood vessels was significantly reduced (Fig. 3*b*). Considering the close relationship between Stx-caused vascular damage in the central nervous system and its mortality in mice (3, 19, 23, 24), these results suggest that SUPER TWIG (1)6 suppressed the lethality of Stx2 by diminishing the deposition of Stx2 in the brain and the subsequent fatal damage.

Next we tested whether SUPER TWIG (1)6 would be effective in protecting mice from death after oral infection with Stx-producing *E. coli* O157:H7. We used mice with protein calorie malnutrition, which are very susceptible to infection with *E. coli* O157:H7 (19). In this model the establishment of infection can be diagnosed by the detection of Stx both in stool on day 2 and in serum on day 3 after an intragastric infection with *E. coli* O157:H7 (19). Using this model, we administered SUPER TWIG (1)6 intravenously twice a day for four consecutive days from day 3 to 6. All of the control animals developed neurologic symptoms after day 5 of infection and succumbed to the infection by day 14 (Fig. 3*c*). In contrast, six of seven mice treated with SUPER TWIG (1)6 survived ($P < 0.01$) more than 40 days without any neurologic symptoms. These results clearly indicate that SUPER TWIG (1)6 can protect mice from a challenge with a fatal dose of *E. coli* O157:H7, even when it is administered after the establishment of an infection.

**Mechanism of Stx-Neutralizing Action of SUPER TWIG (1)6.** Finally, the possible mechanism of Stx2-neutralizing action of SUPER

MICROBIOLOGY

TWIG (1)6 *in vivo* was investigated. First, to examine the effect of SUPER TWIG (1)6 on the tissue distribution of Stx2, we injected $^{125}$I-Stx2 intravenously into mice with or without SUPER TWIG (1)6. One hour after the injection of $^{125}$I-Stx2 alone, 43% of the total radioactivity was recovered from the stomach, and the rest was mostly recovered from the blood, liver, and small intestines (Fig. 4*a*). Coadministration of SUPER TWIG (1)6 with the toxin dramatically changed the distribution of $^{125}$I-Stx2 in that the liver and spleen accumulated the toxin to an extent 3.5 and 5.3 times higher than that observed in the control mice (Fig. 4*a*). On the contrary, the accumulation of radioactivity in the kidney and brain, well known Stx target organs, was reduced by 1.7 and 3.8 times, respectively.

To confirm the SUPER TWIG (1)6-induced accumulation of Stx2 in the liver, we performed an immunohistochemical analysis. In Stx2-injected mice, Stx2 was found to have been deposited in the wall of sinusoids and in red blood cells (Fig. 4*b*). Unexpectedly, in SUPER TWIG (1)6-coinjected mice, the amount of Stx2 protein itself detected by the antibody was substantially reduced in the liver (Fig. 4*b*), although marked accumulation of $^{125}$I radioactivity was observed in the same liver (Fig. 4*a*). Because the liver and spleen are a part of the reticuloendothelial system, it is conceivable that phagocytic macrophages present in these organs had promptly taken up and metabolized Stx2 into small degradation products that could not react with the antibody, when SUPER TWIG (1)6 was administered with the toxin. To test this possibility, we examined SUPER TWIG (1)6-dependent metabolism of Stx2 by using an *in vitro* culture system. In Vero cells, $^{125}$I-Stx2 was effectively incorporated into the cells and further processed to produce its enzymatically active A1 fragment, which causes cell damage, by the action of the membrane-associated protease furin (25) (Fig. 4*c*). This A1 fragment formation was markedly inhibited by an excess of nonlabeled toxin or by SUPER TWIG (1)6. On the contrary, when macrophages prepared from a mouse peritoneal washing were incubated with $^{125}$I-Stx2, $^{125}$I-Stx2 was not incorporated at all in the absence of SUPER TWIG (1)6, but the incorporation of $^{125}$I-Stx2 and the production of the A1 fragment were dramatically accelerated on incubation with SUPER TWIG (1)6 (Fig. 4*c*).

Next, degradation of Stx2 incorporated by macrophages was investigated after the incubation with $^{125}$I-Stx2 in the presence of SUPER TWIG (1)6 for 4 h. The amount of both Stx2 A subunit and A1 fragment produced in cells decreased quickly, and acid-soluble small degradation products were concomitantly released into the culture medium (Fig. 4*d*). These results indicate that macrophages actively incorporated and degraded Stx2 in a SUPER TWIG (1)6-dependent manner. Degradation of the A1 fragment produced in Vero cells was much slower than that observed in macrophages (data not shown). It is plausible, from these results, that SUPER TWIG (1)6 decreases the deposition of Stx2 in pathologically significant target organs such as the brain and kidney by binding to the toxin, and furthermore induces the uptake and immediate degradation of the toxin by phagocytic macrophages present in the reticuloendothelial system in the liver and spleen.

SUPER TWIG (1)12, the most effective SUPER TWIG in the *in vitro* assay, also induced the uptake of $^{125}$I-Stx2 by cultured macrophages; but the efficiency was 3.0 or 2.1 times less (1 or 10 $\mu$g/ml of SUPER TWIG (1)12, respectively) than that of SUPER TWIG (1)6 (Fig. 4*e*). No effect was observed with SUPER TWIG (0)3. These observations might explain in part why SUPER TWIG (1)12 has much less suppressive effect than SUPER TWIG (1)6 on the lethality of Stx2 in mice, although the precise reason remains to be clarified.

In this study, we used a series of carbosilane dendrimers and identified SUPER TWIG (1)6 as a Stx neutralizer that is active in the circulation. Because of their unique characteristics, carbosilane dendrimers make it feasible to optimize the number and the position of the functional terminal trisaccharides, which resulted in SUPER TWIG (1)6, having the most compact structure among all of the Stx neutralizers that have ever been developed (7–10). Furthermore, in the physiological scenario SUPER TWIG (1)6 protected mice from challenge with a fatal dose of *E. coli* O157:H7, even when administered after the establishment of the infection. Therapeutically, this type of neutralizer is expected to have superior advantages to prevent the progression of the life-threatening systemic complications caused by STEC infection, because recent highly sensitive Stx-detection systems make it possible to diagnose the establishment of these infections at a very early stage (4, 19, 24). Also SUPER TWIG (1)6 functions *in vivo* by a unique dual mechanism: (*i*) it binds to Stx with high affinity and inhibits its $Gb_3$-dependent incorporation into target cells; (*ii*) it induces active uptake and subsequent degradation of Stx by macrophages present in the reticuloendothelium. Although the molecular mechanism of the SUPER TWIG-dependent incorporation of Stx by macrophages remains to be elucidated, this type of neutralizer provides a strategy to eliminate harmful materials from the body. The method presented here should be widely applicable for the design of highly selective inhibitors for other bacterial toxins and also for viruses that infect cells by way of carbohydrate receptors.

We thank Dr. Shinji Yamasaki for providing us with the pUC118 vector containing the complete coding sequence of Stx1, and Drs. Hiroyuki Arai and Yoshifumi Takeda for their continuous encouragement and fruitful discussion. This work was supported in part by Health Sciences Research Grant on Emerging and Re-emerging Infectious Diseases H12-E-25 and International Health Cooperation Research Grant 11-S-1 from the Ministry of Health, Labor and Welfare, Japan.

1. Karmali, M. A., Steele, B. T., Petric, M. & Lim, C. (1983) *Lancet* **i**, 619–620.
2. Riley, L. W., Remis, R. S., Helgerson, S. D., McGee, H. B., Wells, J. G., Davis, B. R., Hebert, R. J., Olcott, E. S., Johnson, L. M., Hargrett, N. T., *et al.* (1983) *N. Engl. J. Med.* **308**, 681–685.
3. O'Brien, A. D. & Holmes, R. K. (1987) *Microbiol. Rev.* **51**, 206–220.
4. Paton, J. C. & Paton, A. W. (1998) *Clin. Microbiol. Rev.* **11**, 450–479.
5. Karmali, M. A., Petric, M., Lim, C., Fleming, P. C., Arbus, G. S. & Lior, H. (1985) *J. Infect. Dis.* **151**, 775–782.
6. Melton-Celsa, A. R. & O'Brien, A. D. (1998) in *Escherichia coli O157:H7 and Other Shiga Toxin-Producing E. coli Strains*, eds. Kaper, J. B. & O'Brien, A. D. (Am. Soc. Microbiol., Washington, DC), pp. 121–128.
7. Armstrong, G. D., Fodor, E. & Vanmaele, R. (1991) *J. Infect. Dis.* **164**, 1160–1167.
8. Kitov, P. I., Sadowska, J. M., Mulvey, G., Armstrong, G. D., Ling, H., Pannu, N. S., Read, R. J. & Bundle, D. R. (2000) *Nature (London)* **403**, 669–672.
9. Dohi, H., Nishida, Y., Mizuno, M., Shinkai, M., Kobayashi, T., Takeda, T., Uzawa, H. & Kobayashi, K. (1999) *Bioorg. Med. Chem.* **7**, 2053–2062.
10. Paton, A. W., Morona, R. & Paton, J. C. (2000) *Nat. Med.* **6**, 265–270.
11. Matsuoka, K., Terabatake, M., Esumi, Y., Terunuma, D. & Kuzuhara, H. (1999) *Tetrahedron Lett.* **40**, 7839–7842.
12. Noda, M., Yutsudo, T., Nakabayashi, N., Hirayama, T. & Takeda, Y. (1987) *Microb. Pathog.* **2**, 339–349.
13. Kurazono, H., Sasakawa, C., Yoshikawa, M. & Takeda, Y. (1987) *FEMS Microb. Lett.* **44**, 23–26.
14. Goldstein, J. L., Basu, S. K. & Brown, M. S. (1983) *Methods Enzymol.* **98**, 241–260.
15. Nishikawa, K., Arai, H. & Inoue, K. (1990) *J. Biol. Chem.* **265**, 5226–5231.
16. Yamasaki, C., Natori, Y., Zeng, X.-T., Ohmura, M., Yamasaki, S., Takeda, Y. & Natori, Y. (1999) *FEBS Lett.* **442**, 231–234.
17. Plant, A. L., Brigham-Burke, M., Petrella, E. C. & O'Shannessy, D. J. (1995) *Anal. Biochem.* **226**, 342–348.
18. Mizuguchi, M., Tanaka, S., Fujii, I., Tanizawa, H., Suzuki, Y., Igarashi, T., Yamanaka, T., Takeda, T. & Miwa, M. (1996) *Acta Neuropathol.* **91**, 254–262.
19. Kurioka, T., Yunou, Y. & Kita, E. (1998) *Infect. Immun.* **66**, 1726–1734.
20. Ling, H., Boodhoo, A., Hazes, B., Cummings, M. D., Armstrong, G. D., Brunton, J. L. & Read, R. J. (1998) *Biochemistry* **37**, 1777–1788.
21. Takeda, Y., Kurazono, H. & Yamasaki, S. (1993) *Microbiol. Immunol.* **37**, 591–599.
22. Richardson, S. E., Rotman, T. A., Jay, V., Smith, C. R., Becker, L. E., Petric, M., Olivieri, N. F. & Karmali, M. A. (1992) *Infect. Immun.* **60**, 4154–4167.
23. Fujii, J., Kita, T., Yoshida, S.-I., Takeda, T., Kobayashi, H., Tanaka, N., Ohsato, K. & Mizuguchi, Y. (1994) *Infect. Immun.* **62**, 3447–3453.
24. Kita, E., Yunou, Y., Kurioka, T., Harada, H., Yoshikawa, S., Mikasa, K. & Higashi, N. (2000) *Infect. Immun.* **68**, 1207–1214.
25. Garred, O., van Deurs, B. & Sandvig, K. (1995) *J. Biol. Chem.* **270**, 10817–10821.

ELSEVIER

Carbohydrate Polymers 47 (2002) 373–376

Carbohydrate Polymers

www.elsevier.com/locate/carbpol

# Improved solubility of β-cyclodextrin inclusion complexes by using liquid ammonia as a solvent and the possibility of asymmetric reduction

Koji Matsuoka*, Hiroyuki Takahashi, Yosuke Saito, Daiyo Terunuma, Hiroyoshi Kuzuhara

*Department of Functional Materials Science, Faculty of Engineering, Saitama University, Urawa, Saitama 338-8570, Japan*

Received 14 September 2000; revised 5 February 2001; accepted 16 February 2001

**Abstract**

Dramatic improvement in the poor solubility of β-cyclodextrin (β-CD) and its inclusion complexes in water was achieved by using liquid ammonia (liq. $NH_3$) instead of water as the solvent. Asymmetric $NaBH_4$ reduction of the carbonyl groups of the inclusion complexes in liq. $NH_3$ was examined in a homogeneous condition to give the corresponding alcohols with moderate chirality. © 2002 Elsevier Science Ltd. All rights reserved.

*Keywords*: Cyclodextrins; Liquid ammonia; Asymmetric reduction; Inclusion complexes

Cyclodextrins (CDs) are well-known cyclic oligosaccharides composed of several glucose residues linked with *O*-α-D-glucopyranosyl-(1 → 4)-bonds, and they provide a hydrophobic cavity as a functional chiral binding site for hydrophobic guest molecules with the appropriate size for the cavity in aqueous solution (Bender & Komiyama, 1978). Therefore, synthetic approaches to prepare artificial enzymes by means of CDs employed as active sites have been widely investigated (Wenz, 1994; Breslow, 1995). Although β-CD is the most readily available among the CDs and provides an appropriately sized cavity, it shows remarkably poor solubility in water in contrast with other CDs (French, Levine, Pazur & Norberg, 1949). In addition, the inclusion complexes of β-CD with a guest compound are also known to show less solubility in aqueous media. Hitherto, an asymmetric reduction of β-CD inclusion compounds having the carbonyl group employing sodium borohydride ($NaBH_4$) in aqueous suspension has been reported by several groups (Fornasier, Reniero, Scrimin & Tonellato, 1985; Kawajiri & Motohashi, 1989; Sakuraba, Inomata & Tanaka, 1984). Despite the fact that similar conditions were used for the reduction of acetylferrocene, however, the resultant alcohol showed the opposite optical rotations (Fornasier, et al., 1985; Kawajiri & Motohashi, 1989). Since the reaction conditions were heterogeneous due to the low solubility of the β-CD inclusion complex in water, it seems that the asymmetric reduction of the carbonyl group of acetylferrocene did not proceed smoothly and that the yield of the product was therefore poor. In order to enhance the solubility of the inclusion complexes, we have explored possible alternative solvents as completely solvating agents of β-CD inclusion complexes, and we found that liquid ammonia (liq. $NH_3$) is a promising solvent. In this paper, we describe the asymmetric reduction of carbonyl compounds included by β-CD in the presence of $NaBH_4$ in liq. $NH_3$.

One:one stoichiometric inclusion complexes of acetophenone **1** and acetylferrocene **2** with β-CD, respectively, were prepared in water by the usual method, as shown in Fig. 1. A keto acid, 3-(*p*-toluoyl)propionic acid (Burcker, 1988), which is a highly hydrophilic compound, showed high solubility in water even in the presence of the same molar amount of β-CD. Hence, a colorless aqueous solution was evaporated to dryness in order to prepare the inclusion complex **3**. The formation of inclusion complexes was confirmed by examination of $^1H$ NMR spectra of the inclusion complexes. The high magnetic field shifts of H-3 and H-5, respectively, in the β-CD moiety of an inclusion complex from the original chemical shifts of β-CD itself indicated that the guest compound existed near H-3 and H-5 in the hydrophobic cavity of the β-CD moiety. Since the preparation of the inclusion complexes was accomplished, the effectiveness of liq. $NH_3$ as a solvent to dissolve those inclusion complexes was examined. It was found that the inclusion complexes were quickly dissolved in liq. $NH_3$, even when the inclusion complex **2** was added to a stirred solution of liq. $NH_3$. Liq. $NH_3$ proved to be an effective solvent, showing remarkably

* Corresponding author. Tel./fax: +81-48-858-3099.
*E-mail address:* koji@fms.saitama-u.ac.jp (K. Matsuoka).


PII: S0144-8617(01)00189-8

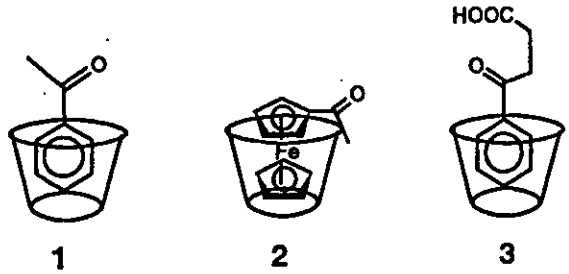


Fig. 1. Structures of guest compounds included by β-cyclodextrin.

improved solubility in comparison with that of water. Thus, liq. $NH_3$ was used as a solvent for asymmetric reduction of the guest compounds included by β-CD.

$NaBH_4$ reduction of a carbonyl compound in order to obtain the corresponding alcohol is generally carried out in an aqueous or alcoholic condition. In the course of our study, $NaBH_4$ reduction of acetophenone without β-CD in liq. $NH_3$ was initially attempted, and the reduction proceeded successfully to afford the corresponding alcohol as a racemate. Therefore, we next attempted the reduction of an acetophenone-β-CD complex **1** by means of $NaBH_4$ in liq. $NH_3$. The reaction was homogeneous and proceeded smoothly to give the corresponding alcohol **4** having $[\alpha]_D^{25} = -0.19°$ (~0% ee) in 66% chemical yield, as shown in Fig. 2. On the other hand, 1-ferrocenylethanol **5** (Gokel, Marquarding & Ugi, 1972) having $[\alpha]_D^{25} = -3.68°$ (12% ee) was isolated from the reaction mixture of the acetylferrocene-β-CD complex **3** with $NaBH_4$ in liq. $NH_3$ in 74% chemical yield. These results suggest that in the reaction with **1**, the hydride simultaneously attacks the carbonyl carbon from both sides without any influence from the hydrogen bond caused by β-CD, as shown in Fig. 3(A), while in the reaction with **2**, an influence of β-CD through the hydrogen bond between the hydroxy group of the β-CD and the carbonyl oxygen atom of the acetylferrocene was observed (Fig. 3(B)). Consequently, the hydride could attack the carbocation from the opposite side to β-CD to provide an alcohol with an (*R*)-(−) configuration as the sole product. This finding is consistent with the fact that the acetylferrocene molecule is accommodated in the cavity of β-CD by axial orientation (Harada & Takahashi, 1984), and therefore the reduction of the acetylferrocene showed stereochemical results. In addition, the stereoselectivity of the reduction of the acetylferrocene supports the result obtained by Kawajiri and Matsuhashi using aqueous media (Kawajiri & Motohashi, 1989).

As the $NaBH_4$ reduction of carbonyl compounds included by β-CD in liq. $NH_3$ was successful, we turned our attention toward the reduction of a keto acid, such as 3-(*p*-toluoyl)-propionic acid, in which the carboxylic group is highly hydrophilic. In our previous study, reduction of an α-keto acid, phenyl pyruvic acid, was attempted using the same strategy as that employed for **1** and **2**. Although the reaction proceeded smoothly, isolation of the product from the reaction mixture was unsuccessful due to the high solubility of the alcohol in water. For that reason, a γ-keto acid as the precursor of γ-hydroxy acid, which can be converted into its lactone with less hydrophilicity by a $H^+$-mediated lactonization, was selected for the application of $NaBH_4$ reduction in liq. $NH_3$. Thus, the $NaBH_4$ reduction in liq. $NH_3$ of **3** followed by the lactonization in the presence of HCl gave lactone **6** as the enantiomeric mixture quantitatively in Scheme 1. To determine the enantiomeric excess of the product by optical resolution, further manipulation by using (*S*)-(−)-1-phenylethylamine to **6** was attempted. The amidation gave a diastereomeric mixture **7**, and the enantiomeric excess of the resultant diastereomer was estimated to be 2.6% ee as judged by the area ratio in the HPLC profile as shown in Fig. 4. Therefore, despite the fact that the $NaBH_4$ reduction of 3-(*p*-toluoyl)propionic acid included by β-CD proceeded smoothly in liq. $NH_3$, the resulting lactone **6**, however, had very limited chirality. Since this stereochemistry was close to that of **1**, we speculate that a hydride attack occurred at the carbocation from both sides.

In conclusion, the use of liq. $NH_3$ instead of water as a solvent to create a homogeneous solution of β-CD inclusion complexes was found to be efficient and useful. Asymmetric reduction of the carbonyl group of the guest compounds included by β-CD in liq. $NH_3$ in the presence of $NaBH_4$ proceeded homogeneously to provide the corresponding alcohols with limited chirality.

## 1. Experimental

### *1.1. Materials and methods*

Unless otherwise stated, all commercially available solvents and reagents were used without further purification. Melting points were measured with a Laboratory Devices MELTEMP II apparatus and were uncorrected. The optical rotations were determined with a JASCO DIP-1000 digital polarimeter. The IR spectra were obtained using a JASCO FT/IR-300E spectrophotometer. The $^1H$ NMR spectra were recorded at 400 MHz with a Bruker AM-400 spectrometer or at 200 MHz with a Varian Gemini-2000 spectrometer in chloroform-*d* or deuterium oxide. Tetramethylsilane (TMS) or methanol (3.3 ppm) were used as internal standards. Ring-proton assignments in NMR were made on the basis of the

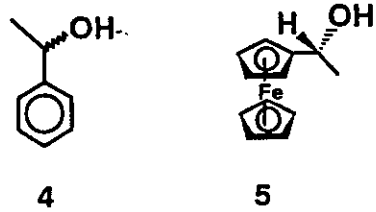


Fig. 2. Structures of isolated alcohols produced by $NaBH_4$ reduction in liq. $NH_3$.

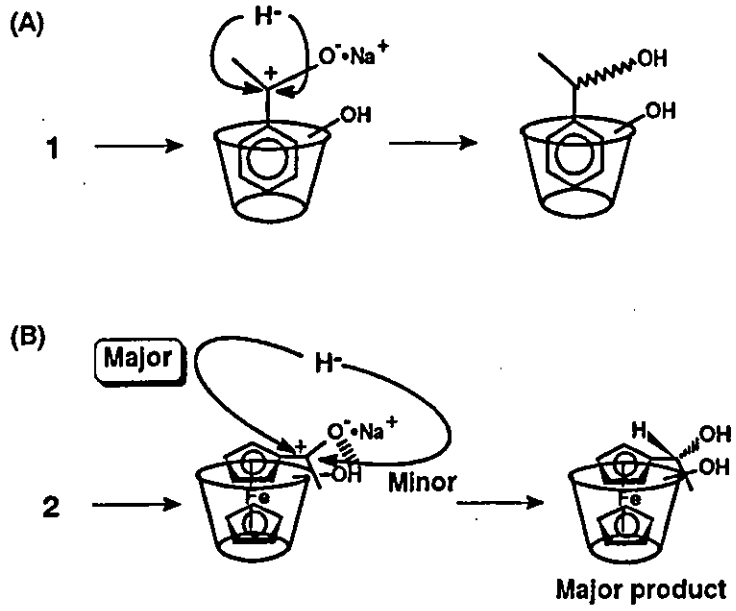


Fig. 3. Proposed mechanism for asymmetric reduction of the carbonyl compound included by β-CD.

results of first-order analysis of the spectra, and the assignments were supported by the results of homonuclear decoupling experiments. Reactions were monitored by thin-layer chromatography (TLC) on a precoated plate of silica gel $60F_{254}$ (layer thickness, 0.25 mm; E. Merck, Darmstadt, Germany). For detection of the intermediates, TLC sheets were sprayed with: (a) a solution of 85:10:5 (v/v/v) methanol-*p*-anisaldehyde-concentrated sulfuric acid and heated for a few minutes (for carbohydrate) or (b) an ethanolic solution of 7% phosphomolybdic acid and heated similarly. Column chromatography was performed on silica gel (Silica Gel 60; 63–200 μm, E. Merck). All extractions were concentrated below 45°C under diminished pressure. HPLC was performed using a Finepak SIL column (0.46 mm × 250 mm, JASCO) at ambient temperature. The column was equilibrated with hexane–ethyl acetate (6:4, v/v) and run at a flow rate of 1.0 ml/min. For the detection of the sample on HPLC, UV 254 nm was used.

*1.2. Preparation of inclusion complexes of β-CD with guest molecules*

*β-CD–acetophenone complex* (**1**). To a stirred solution of β-CD (10.15 g, 7.5 mmol) in water (550 ml) was added dropwise acetophenone (901 mg, 7.5 mmol) at rt. After 7 h, the reaction mixture was cooled to 4°C and left for 22 h. Resulting crystals were collected by filtration, washed with diethyl ether, and dried in vacuo to give white powdery **1** (5.84 g, 62%): IR (KBr) 3368 ($\nu_{O-H}$), 1686 ($\nu_{C=O}$) $cm^{-1}$.

*β-CD–acetylferrocene complex* (**2**). To a solution of β-CD (5.00 g, 4.4 mmol) in water (275 ml) was added a solution of acetylferrocene (1.00 g, 4.4 mmol) in diethyl ether (20 ml) at rt with stirring. The resulting mixture was stirred for 6 h at rt and then left for 2 h at 4°C. The orange-colored crystals were filtered off, washed with diethyl ether, and dried in vacuo to afford **2** (5.09 g, 85%): IR (KBr) 3349 ($\nu_{O-H}$), 1673 ($\nu_{C=O}$) $cm^{-1}$.

*β-CD–3-(p-toluoyl)propionic acid complex* (**3**). 3-(*p*-Toluoyl)propionic acid (Burcker, 1988) (1.19 g,

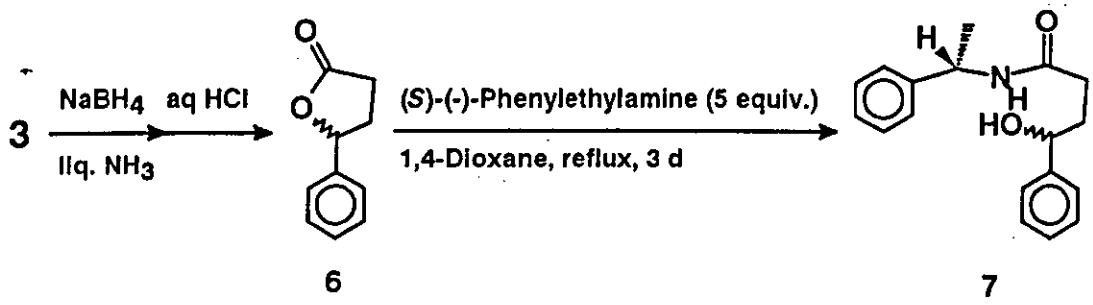


Scheme 1.

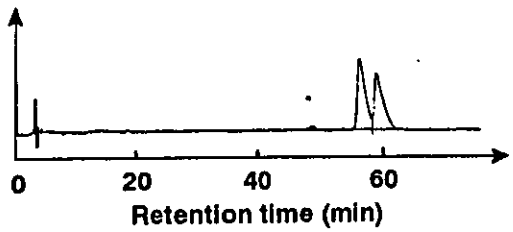


Fig. 4. HPLC profile of 7 as a diastereomeric mixture. 7 was injected into an optical resolution column. Elution conditions are described in the Section 1.

6.16 mmol) was added to a solution of β-CD (7.00 g, 6.16 mmol) in water (1540 ml) with stirring. The solution was further stirred for 18 h at rt, and the resulting mixture was evaporated in vacuo to give **3** (7.36 g, 90%) as white powder: IR (KBr) 3370 ($\nu_{O-H}$), 1684 ($\nu_{C=O}$) $cm^{-1}$, $^1H$ NMR $\delta$ (400 MHz, $D_2O$) 2.44 (s, 3H, Ph-C*H*$_3$), 2.76 (t, 2H, $J = 6.5$ Hz, $CH_2$), 3.36 (m, 2H, $CH_2$), 3.59 (t, 7H, $J_{3,4} = J_{4,5}$ 9.5 Hz, H-4), 3.65 (dd, 7H, $J_{1,2} = 3.6$ Hz and $J_{2,3} = 10.0$ Hz, H-2), 3.74 (dt, 7H, H-5), 3.86–3.92 (m, 21H, H-3 and H-6), 5.07 (d, 7H, H-1), 7.41 (d, 2H, $J = 7.9$ Hz, Ph-*H*), 7.93 (d, 2H, $J = 8.2$ Hz, Ph-*H*).

*Reduction of acetophenone included by β-CD* (**1**). Inclusion complex **1** (3.00 g, 2.39 mmol) was added three-portionwise to liq. $NH_3$ at ca. −40°C, giving a clear solution. To this solution was added $NaBH_4$ (226 mg, 5.98 mmol), and the solution was stirred for 2 days at ca. −40°C. After evaporation of $NH_3$, water (30 ml) was added to the resulting mixture, and the solution was then cooled to 0°C. To the cooled solution was added 1 M aq. HCl [6 mL, (1 M = 1 mol $dm^{-3}$)] and then $CHCl_3$ (400 ml), and the mixture was stirred for 18 h. The mixture was filtered, and the insoluble mass was further extracted using chloroform (100 ml and 200 ml) with stirring. The filtrate and extracts were combined, partitioned, dried over anhydrous sodium sulfate, and concentrated to provide **4** as a colorless syrup: $[\alpha]_D^{25} = +0.19°$ (*c* 1.39, $CHCl_3$), IR (neat) 3365 ($\nu_{O-H}$), 3085, 3061, 3029 ($\nu_{C-H}$) $cm^{-1}$.

*Reduction of acetylferrocene included by β-CD* (**2**). $NaBH_4$ (315 mg, 8.33 mmol) was added to a solution of **2** (0.50 g, 2.20 mmol) in liq. $NH_3$ (250 ml) at ca. −40°C, and the solution was stirred for 2 days at the same temperature. After removing $NH_3$, the residue was diluted with water (50 ml), 1 M aq. HCl (8 ml), and $CHCl_3$ (400 ml). The mixture was stirred for 23 h at rt. The mixture was filtered and the filtrate was partitioned. The insoluble mass was further extracted with chloroform (twice) overnight with continuos stirring, then filtered. Both of the $CHCl_3$ solutions were combined, evaporated, and dried in vacuo to give orange-colored **5** (375 mg, 74%): mp 61–68°C; $[\alpha]_D^{27} = -3.68°$ (*c* 2.47, $CHCl_3$), IR (KBr) 3213 ($\nu_{O-H}$), 3087 ($\nu_{C-H}$) $cm^{-1}$.

*Reduction of 3-(p-toluoyl)propionic acid included by β-CD* (**3**). A solution of **3** (3.00 g, 2.26 mmol) and $NaBH_4$ (210 mg, 5.65 mmol) in liq. $NH_3$ (250 ml) was stirred for 2 days at ca. −40°C. Liq. $NH_3$ was evaporated, and the residue was treated with 6 M aq. HCl (40 ml) and $CHCl_3$ (400 ml) with stirring for 20 h at rt. The resulting mixture was filtered, and the filtrate was partitioned. The organic layer was washed with water and concentrated to afford **6** as white crystals: mp 70–71°C, $[\alpha]_D^{28} = +1.23°$ (*c* 1.99, $CHCl_3$), IR (KBr) 3040 ($\nu_{O-H}$), 1766 ($\nu_{C=O}$) $cm^{-1}$, $^1H$ NMR $\delta$ (200 MHz, $CDCl_3$) 2.21 (m, 2H, $CH_2$), 2.36 (s, 3H, Ph-C*H*$_3$), 2.65 (m, 2H, $CH_2$), 5.48 (m, 1H, CH), 7.17–7.24 (m, 4H, 4Ph-*H*).

*(S)-1-Phenylethylamidation of* **6**. A mixture of **6** (100 mg, 0.57 mmol) and (S)-(−)-1-phenylethylamine (345 mg, 2.85 mmol) in 1,4-dioxane (1.0 ml) was stirred at 100°C for 68 h. After evaporation, the residue was diluted with $CHCl_3$. The $CHCl_3$ solution was successively washed with 5% aq. sulfuric acid, saturated sodium hydrogen bicarbonate, and water, then dried over anhydrous sodium sulfate, filtered, and concentrated. The residue was chromatographed on silica gel with toluene–ethyl acetate (2:1, v/v) as the eluent to give amide **7** as light-yellow crystals: mp 96–98°C, $[\alpha]_D^{22} = -70°$ (*c* 2.29, $CHCl_3$), IR (KBr) 3558 ($\nu_{O-H}$), 3306 ($\nu_{N-H}$), 3064, 3030 ($\nu_{C=H}$), 1646 ($\nu_{C=O}$), 1543 ($\delta_{N-H}$) $cm^{-1}$, $^1H$ NMR $\delta$ (400 MHz, $CDCl_3$) 1.43 (d, 3H, $J = 6.9$ Hz, PhCHC*H*$_3$), 1.99 (m, 2H, $CH_2$), 2.27 (m, 2H, $CH_2$), 2.32 (s, 3H, Ph-C*H*$_3$), 3.79 (br d, 1H, $J = 10.7$ Hz, OH), 4.65 (m, 1H, $CH_2CH$), 5.07 (m, 1H, MeC*H*), 6.18 (br s, 1H, NH), 7.10–7.33 (m, 9H, 9Ph-*H*).

## References

Bender, M. L., & Komiyama, M. (1978). *Cyclodextrin chemistry*, New York: Springer (and references cited therein).

Breslow, R. (1995). Biomimetic chemistry and artificial enzymes: catalysis by design. *Accounts of Chemical Research, 28*, 146–153.

Burcker, M. E. (1888). *Bulletin de la Societe Chimique de Paris, 49*, 448.

Fornasier, R., Reniero, F., Scrimin, P., & Tonellato, U. (1985). Asymmetric reductions by $NaBH_4$ of ketone — β-cyclodextrin complexes. *Journal of Organic Chemistry, 50*, 3209–3211.

French, D. L., Levine, M., Pazur, J. H., & Norberg, E. (1949). Studies on the Schardinger dextrins: the preparation and solubility characteristics of alpha, beta, and gamma dextrins. *Journal of American Chemical Society, 71*, 353–356.

Gokel, G. W., Marquarding, D., & Ugi, I. K. (1972). The retentive nucleophilic displacements of α-substituted alkylferrocenes. *Journal of Organic Chemistry, 37*, 3052–3058.

Harada, A., & Takahashi, S. (1984). Preparation and properties of cyclodextrin–ferrocene inclusion complexes. *Journal of Chemical Society, Chemical Communications*, 645–646.

Kawajiri, Y., & Motohashi, N. (1989). Strong asymmetric induction without covalent bond connection. *Journal of Chemical Society, Chemical Communications*, 1336–1337.

Sakuraba, H., Inomata, N., & Tanaka, Y. (1984). Asymmetric reduction of ketones with crystalline cyclodextrin complexes of amine–boranes. *Journal of Organic Chemistry, 54*, 3482–3484.

Wenz, G. (1994). Cyclodextrin as binding blocks for supramolecular structures and functional units. *Angewandte Chemie International Edition in English, 33*, 803–822.